FEMS Microbiology Ecology, 92, 2016, fiw018

doi: 10.1093/femsec/fiw018
Advance Access Publication Date: 31 January 2016
Research Article

RESEARCH ARTICLE

Microbial diversity in European alpine permafrost and active layers

Beat Frey[1], Thomas Rime[1], Marcia Phillips[2], Beat Stierli[1], Irka Hajdas[3], Franco Widmer[4] and Martin Hartmann[1,*]

[1]Forest Soils and Biogeochemistry, Swiss Federal Research Institute WSL, Birmensdorf, Switzerland, [2]Snow and Permafrost, WSL Institute for Snow and Avalanche Research SLF, Davos, Switzerland, [3]Laboratory of Ion Beam Physics, Swiss Federal Institute of Technology ETH Zurich, Zurich, Switzerland and [4]Institute for Sustainability Sciences, Agroscope, Zurich, Switzerland

*Corresponding author: Swiss Federal Institute for Forest, Snow and Landscape Research WSL, Zuercherstrasse 111, CH-8903 Birmensdorf, Switzerland. Tel: +41-44-739-2807; Fax: +41-44-739-2215; E-mail: martin.hartmann@wsl.ch

One sentence summary: Permafrost harbours novel microbial diversity featuring species with poorly understood adaptation mechanisms to sub-zero conditions, which has important implications for our understanding of the biological dynamics in a warming world.

Editor: Rosa Margesin

ABSTRACT

Permafrost represents a largely understudied genetic resource. Thawing of permafrost with global warming will not only promote microbial carbon turnover with direct feedback on greenhouse gases, but also unlock an unknown microbial diversity. Pioneering metagenomic efforts have shed light on the permafrost microbiome in polar regions, but temperate mountain permafrost is largely understudied. We applied a unique experimental design coupled to high-throughput sequencing of ribosomal markers to characterize the microbiota at the long-term alpine permafrost study site 'Muot-da-Barba-Peider' in eastern Switzerland with an approximate radiocarbon age of 12 000 years. Compared to the active layers, the permafrost community was more diverse and enriched with members of the superphylum Patescibacteria (OD1, TM7, GN02 and OP11). These understudied phyla with no cultured representatives proposedly feature small streamlined genomes with reduced metabolic capabilities, adaptations to anaerobic fermentative metabolisms and potential ectosymbiotic lifestyles. The permafrost microbiota was also enriched with yeasts and lichenized fungi known to harbour various structural and functional adaptation mechanisms to survive under extreme sub-zero conditions. These data yield an unprecedented view on microbial life in temperate mountain permafrost, which is increasingly important for understanding the biological dynamics of permafrost in order to anticipate potential ecological trajectories in a warming world.

Keywords: novel microbial diversity; alpine permafrost; Illumina Miseq sequencing; ribosomal markers; bacteria; archaea; eukarya

INTRODUCTION

Permafrost has been defined as lithospheric material (soil, sediment or rock) that is permanently exposed to temperatures below 0°C and remains frozen for at least two consecutive years (Margesin 2009). Permafrost is one of the most extreme environments on Earth, covering more than 20% of the terrestrial surface and representing a significant storage of global carbon (Zimov, Schuur and Chapin 2006; Schuur *et al.* 2008; Zhang *et al.* 2008). There is an increasing concern that global warming leads

Received: 12 November 2015; **Accepted:** 22 January 2016

to widespread thawing of permafrost and a larger seasonally active layer, ultimately promoting microbial turnover of labile organic carbon with direct feedback on the greenhouse gas budget (Schuur *et al.* 2009; Koven *et al.* 2011; DeConto *et al.* 2012). Therefore, much research has focused on incorporating microbial parameters into modelling future scenarios for carbon turnover in these systems (Wagner *et al.* 2007; Hollesen, Elberling and Jansson 2011; Graham *et al.* 2012).

More recently, research activities have focused on detailed characterizations of the microbial communities residing in permafrost as these habitats might lock up a viable, cold-adapted and novel microbial diversity harbouring environmentally and biotechnologically interesting genetic resources with novel metabolic potential (Margesin *et al.* 2008; Margesin and Feller 2010) and, possibly, potentially pathogenic species of environmental concern that will be released into populated areas (Petrova *et al.* 2008; Legendre *et al.* 2014). Culture-dependent approaches have aimed at screening isolates from these communities for activities of interest, including novel degradation pathways, antimicrobial activities or antibiotic resistances. However, we know that only a small minority of the community—typically less than 1% of the total cell counts—can be readily cultured under standard laboratory conditions (Rappe and Giovannoni 2003). Insights into the uncultured fraction have been fuelled by sequencing of microbial ribosomal genes from environmental samples, and this in turn has resulted in the identification of numerous new bacterial phyla, of which many are not represented by cultivated strains (Rinke *et al.* 2013). Recent advances in high-throughput DNA sequencing techniques and metagenomics have provided an unprecedented view on the microbial diversity hidden in permafrost and yielded a better understanding of these extreme habitats (Yergeau *et al.* 2010; Mackelprang *et al.* 2011; Gittel *et al.* 2014; Jansson and Tas 2014; Hultman *et al.* 2015).

Permafrost regions occur at extreme latitudes, but are also frequently found at high elevations and lower latitudes such as the Alps, the Andes or the Himalaya, and can extend down to more than 1000 m into the subsurface (Zhang *et al.* 2008). The phenomenon of permafrost in mountain regions has long been neglected in scientific research and most recent permafrost studies that have harnessed the power of novel DNA sequencing technologies to assess diversity and metabolic potential of microbial communities have focused on permafrost habitats at high latitudes. Altitudinal permafrost habitats feature extreme spatial and geothermal variability, well-drained coarse sediments on steep slopes, snow redistribution by wind and avalanches, warmer mean annual temperatures and a reduced influence of vegetation, making these habitats very different from lowland permafrost at extreme latitudes with distinct responses to climate change (Haeberli and Gruber 2009). Mountain regions at lower latitudes such as the European Alps represent critical watersheds for large areas (Huss 2011) and are densely populated compared to polar regions. Thawing of permafrost will likely have a substantial socio-economic impact on the population in these regions. From a biological perspective, potential impacts not only include natural hazards such as rock avalanches and debris flows, but also rapid dispersal of genetic material locked up in permafrost through river systems along watersheds.

This study represents the first comprehensive three-domain analysis of microbial diversity residing in central European alpine permafrost soils using high-throughput sequencing of ribosomal markers. For this purpose, we gained access to one of the best-studied permafrost sites in the European inner alpine region, where ground temperatures down to a depth of 17 m have been monitored since 1996 (Zenklusen Mutter, Blanchet and Phillips 2010). We applied a unique sampling design to compare soils at the same depths on the south-eastern (SE) and the north-western (NW) slope of the mountain ridge at this site. Most permafrost studies, in particular in plane polar regions, compare the deeper permafrost layer to the overlaying active layer. Although this might be the only option in plane regions, it is potentially problematic as the overlaying layer experiences a stronger influence from external biotic and abiotic factors including influence from vegetation (e.g. root exudation and plant interaction) and climate (e.g. temperature fluctuations, UV radiation and weathering). Therefore, studies comparing the microbial communities in the deeper permafrost layer with the overlaying active layer are, to some degree, confounded by a depth effect. Our approach allows us to directly compare permafrost (NW slope) to non-permafrost soils (SE slope) without the confounding depth effect often inherent to studies in lowland regions at higher latitudes, whereas the close proximity of the sampling pits guarantees similar time of deposition. Therefore, this design adds another component to the exploration of microbial communities in permafrost soils.

MATERIALS AND METHODS

Study site and soil collection

The mountain ridge 'Muot da Barba Peider' was chosen as a study site (Fig. S1a, Supporting Information). This site is located at 2979 m.a.s.l. south-west of Piz Muragl and north-east of Pontresina in the upper Engadine valley (Eastern Swiss Alps). This region has a slightly continental climate with around 1500 mm annual precipitation. Air temperatures measured since 2004 with an onsite automatic weather station range between –25°C and 20°C, with a mean annual air temperature of –3°C. The site is mainly affected by southerly air masses. Maximum annual snow depths ranged between 50 and 300 cm in the measurement period between 2004 and 2014.

The bedrock consists of gneiss from the upper Austroalpine Languard nappe. The flanks of 'Muot da Barba Peider' have a widespread scree cover with a depth of around 1.5–2 m in the upper reaches of the slopes where soil samples were taken. Grain sizes at the surface are blocky, fining downwards. Soil samples were taken on the NW flank of the ridge (791343/152487, 2960 m.a.s.l.) and on its SE flank (791407/152438, 2960 m.a.s.l.). Whereas the near-surface ground on the SE slope is only seasonally frozen, the NW flank is characterized by the presence of continuous permafrost below 1 m depth. Vegetation was equally scarce on both sides of the ridge, basically representing barren soil with some rare individual occurrences of plants (Fig. 1b, Supporting Information), in particular *Poa*, *Cerastium* and *Jacobea* spp.

At the NW slope, the active layer is around 1 m thick and borehole temperature measurements since 1996 show that below the active layer the ground has been permanently frozen down to a depth of at least 17.5m (Fig. S2, Supporting Information; Zenklusen Mutter, Blanchet and Phillips 2010). Whereas near-surface ground temperatures oscillate seasonally (Fig. S2, Supporting Information, blue lines), ground temperatures in deeper layers have increased steadily since 1996 (Fig. S2, Supporting Information, red lines). The volumetric ice content of the scree (determined from borehole cores) is 10%. Beneath the scree, the bedrock contains ice in joints and fissures. The ice originates from precipitation and snowmelt water percolating through the scree and refreezing. Snowmelt water causes rapid

warming of the active layer in spring and simultaneously triggers downslope creep of the entire scree layer (Rist and Phillips 2005). The soils at 'Muot da Barba Peider' are subject to strong diurnal and seasonal temperature variations, with phase changes occurring within the uppermost 1–2 m of the ground. In addition, vertical water fluxes through the scree and along the permafrost table or the surface of the bedrock contribute towards heat transfer and cause annual downslope movements of 5–10 cm in the scree (Phillips, Margreth and Ammann 2003).

In September 2014, bulk soil samples were taken on both flanks of the ridge (Fig. S1a, Supporting Information). On each flank, three soil profiles with a distance of 3 m were excavated up to 160 cm using a shovel exposing a clean vertical profile of over a meter in width. Soil samples were taken at 10 and 160 cm depth. Soil surface was cleaned with sterile spatulas to remove debris and to avoid cross-contamination from upper layers. Each soil layer was randomly subsampled (three replicates) and pooled (containing ∼250 g fresh weight) resulting in a total of 12 soil samples (2 expositions × 2 depths × 3 soil profiles). The spatula was wiped and sterilized with ethanol between different samples. Samples were homogenized in autoclaved bags, stored and transported on dry ice upon arrival in the laboratory. On the NW flank soil, samples were taken from the active layer (10 cm; the layer of ground that is subject to annual thawing and freezing) and the permafrost layer (160 cm), whereas on the SE flank soil samples at both 10 and 160 cm depths are part of the active layer. The four resulting site groups are further termed SE10 (SE slope at 10 cm), SE160 (SE slope at 160 cm), NW10 (NW slope at 10 cm) and NW160 (NW slope at 160 cm). Soil temperature was monitored at the time of sampling. The permafrost layer was characterized with excess segregated ice. Initial processing of the bulk soil included removal of detectable roots prior to homogenizing by sieving (2 mm) the soil fraction of each sample. Soils for DNA extraction were stored in the extraction buffer and kept at –20°C until analysis. Soils for physico-chemical measurements were dried at 60°C and fine grounded.

Soil properties

Soil physico-chemical parameters were analysed as previously described (Zumsteg *et al.* 2012; Zumsteg *et al.* 2013). Gravimetric water content of soils was determined by weighing subsamples before and after drying. Soil pH was determined in water. The soil texture was analysed according to Gee and Bauder (1986) after acid digestion with H_2O_2. For exchangeable metal cations, soil samples were extracted with 1 M NH_4Cl and measured using inductively coupled plasma optical emission spectrometry (ICP-AES; ARL 3580 OPTIMA 3000; Perkin Elmer). The percentage of total organic carbon (TOC) of dried, homogenized soils was measured in duplicate using a TOC analyser (Shimadzu, Tokyo, Japan) after HCl (10%) acid digestion to remove carbonates. Total carbon and total nitrogen contents were measured in duplicates using an automatic element analyser (Shimadzu, Tokyo, Japan).

Radiocarbon measurement

Radiocarbon dating of TOC was performed using the Accelerator Mass Spectrometry facility at the Swiss Federal Institute of Technology (AMS ETH Zurich, Switzerland). Fine ground samples (7–8 mg) were treated with acid (HCl) to remove carbonates (Hajdas 2008). An equivalent of 0.5–1 mg of carbon was placed in tin cups for combustion in an elemental analyser and a subsequent graphitization (Wacker, Němec and Bourquin 2010). ^{14}C concentrations were measured relative to the absolute atmospheric radiocarbon content of the atmosphere in 1950 AD after background correction and δ13C normalization (Hajdas 2008). The ^{14}C ages (BP where 0 BP = AD 1950) were calculated and converted to calendar years (cal. yr BP) using the INTCAL13 calibration curve (Reimer *et al.* 2013).

DNA extraction, target amplification and sequencing

Total genomic DNA was extracted in triplicates from 10 g fresh soil samples using the Ultra Clean Soil DNA Mega Prep kit (MOBIO Laboratories, Inc., Carlsbad, CA, USA) according to the manufacturer's instructions. Triplicate extractions were pooled for downstream analyses. The obtained genomic DNA extracts were quantified using the PicoGreen dsDNA quantitation assay (Invitrogen, Carlsbad, CA) and extracts were stored at −20°C.

The V3-V4 region of the prokaryotic (bacterial and archaeal) small-subunit (16S) rRNA gene was amplified with slightly modified versions of primers 341F (CCTAYGGGDBGCWSCAG, this study) and 806R (GGACTACNVGGGTHTCTAAT, this study). The internal transcribed spacer region 2 (ITS2) of the eukaryotic (fungal and some groups of protists and green algae) ribosomal operon was amplified with degenerate versions of primers ITS3 (CAHCGATGAAGAACGYRG) and ITS4 (TCCTSCGCTTATTGATATGC) according to Tedersoo *et al.* (2014). The 5′ ends of the primers were tagged with the CS1 (forward) and CS2 (reverse) adapters required for multiplexing samples using the Fluidigm Access Array System (Fluidigm, South San Francisco, CA, USA). PCR amplification was performed in a total volume of 50 μl reaction mixture containing 40 ng (4 ng for lower depths) of template DNA, 1x PCR-buffer (Qiagen, Hilden, Germany), 2 mM $MgCl_2$, 0.2 mM of each primer, 0.4 mM deoxynucleoside triphosphate (Promega, Dübendorf, Switzerland), 0.6 mg ml^{-1} BSA (Fluka, Buchs, Switzerland) and 2 U HotStar Taq polymerase (Qiagen). The PCR conditions to amplify the prokaryotic 16S and eukaryotic ITS2 fragments consisted of an initial denaturation at 95°C for 10 min, 38 (16S) or 42 (ITS2) cycles of denaturation at 95°C for 40 s, annealing at 58°C for 40 s and elongation at 72°C for 1 min followed by a final elongation at 72°C for 10 min. Each sample was amplified in triplicates and pooled prior to purification with Agencourt AMPure XP beads (Beckman Coulter, Berea, CA) and quantification with the Qubit® 2.0 fluorometric system (Life Technologies, Paisley, UK). Amplicon pools were sent to the Génome Québec Innovation Center at McGill University (Montréal, Canada) for barcoding using the Fluidigm Access Array technology (Fluidigm) and paired-end sequencing on the Illumina MiSeq v3 platform (Illumina Inc., San Diego, CA, USA).

Sequence quality control, OTU clustering and taxonomic assignments

Quality filtering and clustering into operational taxonomic units (OTUs) was performed using a customized pipeline largely based on UPARSE (Edgar 2013; Edgar and Flyvbjerg 2015) implemented in USEARCH v.8 (Edgar 2010), but with some additional modifications. Paired-end reads were merged using the USEARCH fastq_mergepairs algorithm (Edgar and Flyvbjerg 2015), allowing staggered alignment constructs in order to accommodate potentially short ITS2 amplicons. BayesHammer (Nikolenko, Korobeynikov and Alekseyev 2013) was used to correct for substitution errors originating from phasing events during Illumina sequencing. PCR primers were detected and trimmed using Cutadapt (Martin 2011) allowing for one mismatch. Reads not matching the primers or with read lengths below 300 ($16S_{V3V4}$) or 200 bp (ITS2) were discarded. Trimmed reads were

quality-filtered using the USEARCH fastq_filter function with a maximum expected error threshold of one. Sequences were dereplicated to retrieve information on abundance distribution, and singleton reads were removed prior to clustering in order to avoid artificial OTU inflation (Edgar 2013). Sequences were clustered into OTUs at 97% sequence identity using the USEARCH cluster_otu function that includes an 'on-the-fly' chimera detection algorithm (Edgar 2013). OTU centroid sequences were subjected to an additional round of chimera filtering by running UCHIME (Edgar *et al.* 2011) against customized versions of the GREENGENES (DeSantis *et al.* 2006) and UNITE (Nilsson *et al.* 2015) database, respectively. The remaining centroid sequences were tested for the presence of ribosomal signatures using Metaxa2 (Bengtsson-Palme *et al.* 2015) or ITSx (Bengtsson-Palme *et al.* 2013), respectively, and centroid sequences with the ribosomal origin not sufficiently supported were discarded. Finally, all quality-filtered reads were mapped against the final set of centroid sequences using the USEARCH usearch_global algorithm with the most comprehensive search criteria (maxrejects 0, maxaccepts 0 and top_hit_only). Raw sequences have been deposited in the European Nucleotide Archive under the accession number PRJEB11799.

For taxonomic classification of the OTUs, corresponding centroid sequences were queried against selected reference databases using the naïve Bayesian classifier (Wang *et al.* 2007) implemented in MOTHUR (Schloss *et al.* 2009) and a minimum bootstrap support of 60%. Prokaryotic $16S_{V3V4}$ sequences were queried against GREENGENES (DeSantis *et al.* 2006; McDonald *et al.* 2011), whereas eukaryotic ITS2 sequences were first queried against a custom-made ITS2 reference database retrieved from NCBI GenBank (Benson *et al.* 2015) and sequences assigned to fungi were subsequently queried against the fungal ITS database UNITE (Abarenkov *et al.* 2010). Prokaryotic centroid sequences identified as originating from organelles (chloroplast, mitochondria) as well as eukaryotic centroid sequences identified as originating from soil animals (metazoa) or plants (viridiplantae, except green algae), or of unknown eukaryotic origin were removed from downstream analysis.

Statistics

All statistical tests performed in this study were considered significant at $P < 0.05$ unless indicated otherwise. *P*-values were adjusted for multiple testing where necessary by using the Benjamini–Hochberg false discovery rate correction (Benjamini and Hochberg 1995) implemented in the p.adjust function of R (R Core Team 2014) unless indicated otherwise. Differences in soil physico-chemical data were assessed using factorial ANOVA and Tukey's HSD post-hoc test as implemented in R and run in RStudio (RStudio Team 2014). Normal distribution of residues and homogeneity of variance was evaluated using the qqnorm, shapiro.test and leveneTest routines implemented in R (Fox and Weisberg 2011; R Core Team 2014). Non-normal data were transformed where necessary. Overall differences in soil physico-chemical properties were assessed by principal coordinate analysis (PCO; Gower 1966) based on Euclidean distances of z-transformed data. PCOs were calculated using the function cmdscale in R and correlations between the properties and the PCO ordination scores were determined by using the envfit function implemented in the R package vegan (Oksanen *et al.* 2016) with 10^5 permutations. PCOs were plotted in R. Microbial α-diversity was assessed by calculating Shannon diversity indices and rarefaction curves of the observed richness. Shannon diversity indices were calculated using an iterative subsampling procedure based on the samples with the lowest reads counts (54 037 and 11 361 sequences for prokaryotes and eukaryotes, respectively) as implemented in MOTHUR in order to account for differences in read counts across samples. Differences in Shannon diversity among samples were assessed using factorial ANOVA and Tukey's HSD post-hoc test as outlined for the chemical properties above and boxplots were plotted in R. Rarefaction curves were calculated and plotted using the rarecurve function implemented in the R package vegan. Estimates of microbial β-diversity were measured by Bray–Curtis similarities calculated using an iterative subsampling procedure identical to the one described for estimating α-diversity as outlined above. Differences in β-diversity were assessed by PCOs, followed by permutational multivariate analysis of variance (PERMANOVA; Anderson 2001), permutational analysis of multivariate dispersions (PERMDSIP; Anderson 2006) and analysis of similarity (ANOSIM; Clarke 1993) using the homonymous routines in PRIMER6+ (Clarke and Gorley 2006) based on 10^5 permutations (Hartmann *et al.* 2015). Similarities between prokaryotic and eukaryotic β-diversity was assessed by Mantel testing based on the Bray–Curtis dissimilarity matrices and Procrustes analysis based on PCO ordinations using the mantel and protest function, respectively, implemented in vegan with 10^5 permutations. Correlations between physico-chemical properties and the community-based PCO ordination scores were determined by using the envfit function implemented in vegan with 10^5 permutations. The minimal set of physico-chemical soil properties that explains best the variance in community structure was determined using nonparametric multivariate regression between the soil physico-chemical parameters and the OTU-based resemblance matrices implemented as distance-based linear modelling (McArdle and Anderson 2001) in PRIMER6+ and run with 10^5 permutations. Models were built using a step-wise selection procedure and the adjusted R^2 selection criterion. The impact of site and slope on the relative abundance of each phylum was assessed by univariate permutational ANOVA based on Euclidean distances of z-transformed relative abundances and run using the function adonis of the R package vegan with 10^5 permutations. Heatmaps were generated using the function heatmap.2 in the R package gplots based on z-transformed data and included cluster analyses based on the Ward method (Warnes *et al.* 2014).

The association strength of each OTU with a particular site group (i.e. SE10, SE160, NW10 or NW160) or site group combination was determined using correlation-based indicator species analysis (De Cáceres and Legendre 2009) with all possible site combinations (De Cáceres, Legendre and Moretti 2010) as previously described (Hartmann *et al.* 2014, 2015). Indicator species analysis was performed using the multipatt routine implemented in the R package indicspecies (De Cáceres and Legendre 2009) based on 10^5 permutations. *P*-value adjustments for multiple comparisons were performed using the false discovery rate correction according to Storey (2002) implemented in the program QVALITY (Käll, Storey and Noble 2009), and associations were considered significant at $q < 0.05$.

Distribution of OTUs among the different samples was visualized using bipartite network construction with samples as source nodes, OTUs as target nodes and edges representing occurences of particular OTUs in particular samples. The bipartite network was construced using the OpenCL-accelerated Allegro Fruchterman–Reingold algorithm (Fruchterman and Reingold 1991) implemented in CYTOSCAPE (Shannon *et al.* 2003) with edges weighted according to the OTU abundances in the

Table 1. Soil physico-chemical characteristics at the different slopes (SE and NW and depths (10 and 160 cm).

Properties[1]	SE10	SE160	NW10	NW160
C14	4889 ± 76^{A}	$12\,854 \pm 79^{C}$	$12\,923 \pm 149^{C}$	$12\,403 \pm 69^{A}$
C13	-23.8 ± 0.3^{B}	-25.5 ± 0.2^{A}	-20.3 ± 0.2^{C}	-13.8 ± 0.4^{D}
C [%]	0.903 ± 0.035^{C}	0.114 ± 0.009^{B}	0.135 ± 0.009^{B}	0.058 ± 0.004^{A}
N [%]	0.064 ± 0.003	b.d.l.[2]	b.d.l.	b.d.l.
Al [mg kg^{-1} soil]	108.0 ± 2.3^{B}	59.2 ± 0.6^{A}	b.d.l.	b.d.l.
Ca [mg kg^{-1} soil]	5.6 ± 0.2^{A}	8.7 ± 0.1^{A}	675.8 ± 8.5^{B}	869.4 ± 57.7^{C}
Fe [mg kg^{-1} soil]	1.8 ± 0.3	b.d.l.	b.d.l.	b.d.l.
K [mg kg^{-1} soil]	b.d.l.	b.d.l.	44.3 ± 1.8^{B}	34.2 ± 4.0^{A}
Mg [mg kg^{-1} soil]	b.d.l.	b.d.l.	21.3 ± 0.5^{A}	44.2 ± 2.5^{B}
pH [H_2O]	4.6 ± 0.0^{A}	4.8 ± 0.0^{B}	6.5 ± 0.1^{C}	7.4 ± 0.0^{D}
Sand [%]	83.8 ± 0.2^{B}	85.2 ± 0.1^{C}	80.5 ± 0.1^{A}	85.2 ± 0.2^{C}
Silt [%]	14.0 ± 0.3^{C}	13.0 ± 0.3^{B}	15.9 ± 0.2^{D}	11.2 ± 0.4^{A}
Clay [%]	2.2 ± 0.2^{A}	1.8 ± 0.2^{A}	3.6 ± 0.2^{B}	3.5 ± 0.2^{B}

[1]Values represent means ± standard deviations ($n = 3$). Different letters indicate significant ($P < 0.05$) differences between individual means assessed by two-way factorial analysis of variance (ANOVA) followed by Tukey's HSD post-hoc testing. Abbreviations: C14, carbon isotope 14C; C13, carbon isotope 13C; C, carbon; N, nitrogen; Al, aluminum; Ca, calcium; Fe, iron; K, potassium; Mg, magnesium.
[2]b.d.l., below detection limit (i.e. N < 0.015, Al < 0.1, Fe < 0.08, K < 1.6 and Mg < 0.2).

corresponding samples. Directed networks visualizing the OTU distribution across the taxonomic hierarchy (Hartmann *et al.* 2014; Hartmann *et al.* 2015) were generated based on the taxonomic path of each OTU and the OpenCL-accelerated Allegro Fruchterman–Reingold algorithm in CYTOSCAPE with networks split by phyla.

RESULTS

Soil chemistry

Soil physico-chemical properties strongly differed between the two slopes and the two soil layers (Table 1; Fig. S3, Supporting Information). Data on soil chemistry indicated higher biological activity in the upper layer at the SE slope of the ridge, when compared to the NW slope as well as the deeper layers at both sites (Table 1). SE10 revealed highest carbon and nitrogen contents as well as lowest pH and mineral nutrients such as calcium, magnesium and potassium. The permafrost layer in the north (NW160) basically represented the other end of the spectrum. The ^{14}C age, as a measure of carbon turnover in the system, was around 5000 years in SE10 and around 13 000 years in the three other more inactive sites. Higher content of NH_4Cl-exchangeable aluminum and iron in SE10 indicated stronger weathering on the SE slope. The magnitude of differences in edaphic properties between the upper and lower layer was similar at both slopes (Fig. S3, Supporting Information).

Microbial diversity

Sequencing yielded a total of 748 931 (62 411 ± 6 622 per sample) prokaryotic $16S_{V3V4}$ and 776 434 (64 703 ± 27 309) eukaryotic ITS2 high-quality sequences that were clustered into 3431 (1233 ± 693) and 906 (204 ± 93) OTUs, respectively. Slope (SE or NW) and depth (10 or 160 cm) were significant determinants of microbial diversity at this site (Fig. 1). Shannon diversity indices indicated higher α-diversity on the NW slope with the highest diversity in the permafrost layer (Fig. 1a). Rarefaction curves indicated that these differences were better supported for prokaryotes than eukaryotes (Fig. 1a), largely, because sequence coverage for eukaryotes in NW10 samples was reduced by the presence of substantial amounts of plant DNA (*Cerastium fontanum*, *Poa laxa* and *Jacobaea carniolica*) in the ITS2 amplicon libraries. Slope and depth explained 88% (prokaryotes) and 79% (eukaryotes) of the variability in microbial β-diversity, leaving only 12%–21% unexplained (Table 2). Communities were distinct among all four sites, but differences between the upper and lower layers were much smaller in SE than NW (Fig. 1b). Differences in prokaryotic and eukaryotic community structures were very similar as determined by Mantel testing ($r = 0.89$; $P < 0.00001$) and PCO-based Procrustes analysis ($m = 0.14$; $P < 0.00009$). Distance-based linear modelling revealed that the set of pH (explaining 59% of the variance), potassium (23%) and aluminum (9%) best explain the variance in prokaryotic community structure. For eukaryotes, the model determined the properties magnesium (41%), sand (21%) and ^{14}C (14%) as the minimum set of best predictors.

The most abundant bacterial groups across all samples included candidate phylum AD3 (20%), Proteobacteria (18%), Verrucomicrobia (13%), Acidobacteria (12%), OD1 (9%), Chloroflexi (7%), Planctomycetes (5%), Actinobacteria (4%), Gemmatimonadetes (4%), Bacteroidetes (2%) and Nitrospirae (1%); all other groups had a relative abundance below 1% (Table 3; Fig. 1c). Only few archaeal sequences (0.5%) were detected in this dataset. The most abundant eukaryotic groups included the fungal phyla Ascomycota (46%), the former Zygomycota (22%) and Basidiomycota (7%), as well as Alveolata (6%) and Chlorophyta (3%). Notably, a larger fraction of the fungal sequences were not assigned beyond the fungal kingdom (14%). However, there were large differences in relative abundances at the phylum level with some highly abundant groups being only abundant at certain sites and almost all groups were influenced by slope and/or depth (Figs 1c and d, Fig. 2; Table 3). Here, we report on the most salient cases. For example, bacterial candidate phylum AD3 was substantially more abundant at the SE slope (39% at SE versus 1% at NW), whereas candidate OD1 was almost exclusively detected at the NW slope (19% at NW versus 0.2% at SE). Indicator species analysis revealed that OD1 was significantly associated with the permafrost layer, making up more than one fourth of the total community in these samples (Table 3). It was striking that many undercharacterized bacterial phyla with few or no cultured representatives such as OD1 (proposed as Parcubacteria), TM7 (Saccharibacteria), GN02 also known as BD1-5 (Gracilibacteria), OP11 (Microgenomates), SR1, MVP-21, WS5, OP5 (Caldiserica) and Kazan-3B-28, or even entirely unclassified bacteria were enriched in the permafrost soils, whereas other candidates such as WS3 (Latescibacteria), TM6, WS2, OP10

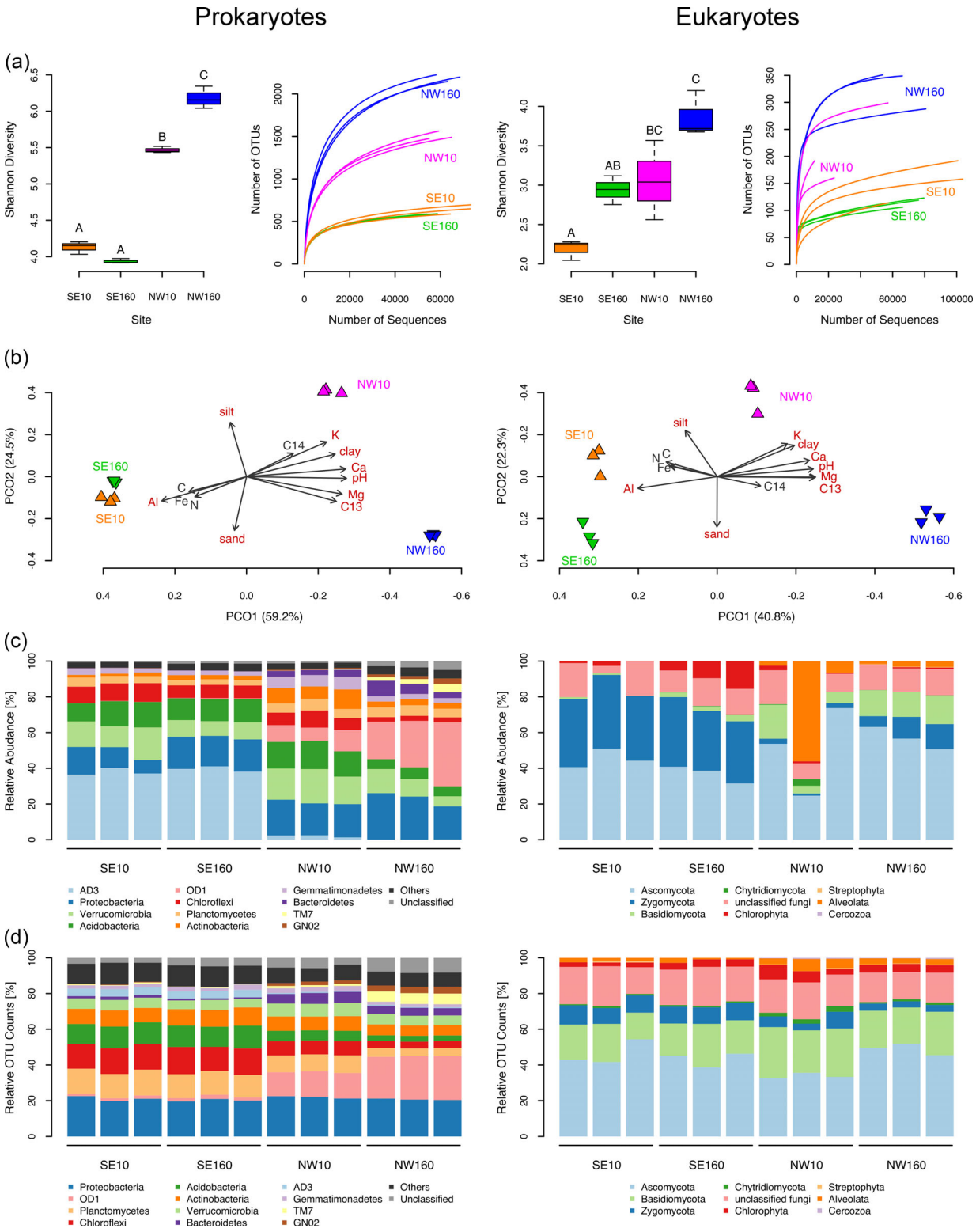

Figure 1. Differences in prokaryotic (left panel) and eukaryotic (right panel) community structure at the different slopes and depths. (**a**) Microbial α-diversity was assessed by calculating Shannon diversities and rarefaction curves of the observed richness. Boxplots include the medians (horizontal lines), interquartile ranges (boxes) and maximal/minimal values (whiskers) of the Shannon diversity indices. Different letters indicate differences ($P < 0.05$) between individual means as assessed by two-way factorial ANOVA followed by Tukey's HSD post-hoc testing. (**b**) Differences in microbial β-diversity among samples were assessed by analysis of principal coordinates (PCO) based on Bray–Curtis dissimilarities. The variance explained by each PCO axis is given in parentheses. Quantitative statistics based on permutational ANOVA are provided in Table 2. Vectors represent correlations of soil physico-chemical parameters with the PCO ordination scores with the significant ($P < 0.05$) correlations in red. (**c**) Relative abundances of most predominant phyla (or other eukaryotic supergroups of no official rank such as Alveolata and Rhizaria). (**d**) Relative OTU counts of the most diverse (in terms of OTU richness) phyla (or other eukaryotic supergroups of no official rank such as Alveolata and Rhizaria). Note: *Nitrospirae* were slightly more abundant than TM7 and GN02, but for the purpose of consistency with panel d, they were merged with the group 'Others' in panel c.

Table 2. Changes in prokaryotic and eukaryotic community structure between the different slopes (SE and NW) and depths (10 and 160 cm).

	Prokaryotes			Eukaryotes		
Main test	F	P	ECV [%]	F	P	ECV [%]
Slope	55.5	0.00001	38	12.6	0.00001	29
Depth	15.6	0.00008	19	7.8	0.00030	22
Slope × Depth	18.8	0.00002	30	6.0	0.00140	27
Pairwise tests	t	P	BC [%]	t	P	BC [%]
SE10 versus SE160	3.2	0.00730	45	3.0	0.01460	69
SE10 versus NW10	4.9	0.00144	85	2.1	0.02980	84
SE10 versus NW160	5.7	0.00140	97	4.3	0.00600	96
SE160 versus NW10	6.3	0.00140	80	2.5	0.02016	90
SE160 versus NW160	8.0	0.00120	96	5.3	0.00600	95
NW10 versus NW160	4.7	0.00144	77	2.5	0.02016	89

Effects of slope, depth, and their interactions as assessed by multivariate permutational ANOVA (PERMANOVA). Values represent the pseudo-F ratio (F) for the main tests and the univariate *t*-statistic (t) for the pairwise tests, the Monte Carlo approximated level of significance (P), the estimated components of variance (ECV) for the main factors, and the average between-group Bray–Curtis dissimilarity (BC) between pairs. *P*-values from pairwise tests were adjusted for multiple comparisons using the Benjamini–Hochberg procedure.

(Armatimonadetes), OP3 (Omnitrophica), NKB19 (Hydrogenedentes) or BRC1 were significantly associated with both NW layers or only NW10. Among better-known phyla with cultured representatives, Chlamydiae were significantly associated with the permafrost layer, Bacteroidetes were more abundant in both NW layers, and Actinobacteria as well as Gemmatimonadetes were abundant in NW10. Proteobacteria tended to be more abundant in the NW, especially in the permafrost, but statistics only demonstrated a lower abundance in SE10 compared to the other sites. Chloroflexi and Acidobacteria were significantly less abundant in the permafrost compared to the other three habitats. Verrucomicrobia were more abundant in the upper layers independent of the slope, and Nitrospirae as well as green algae (Chlorophyta) were characteristic of the lower soil layer at the SE slope. As for the archaea, Thaumarchaeota were more abundant at the SE slope, whereas Euryarchaeota were more abundant at the NW slope with no differences between the two depths. With respect to fungi, Zygomycota were more abundant at the SE slope, whereas Basidiomycota were more abundant at the NW slope. The protistan groups Ciliophora (Alveolata) and Cercozoa (Rhizaria) tended to be more abundant in the NW, but their distribution across samples was rather patchy. Finally, Ascomycota and Firmicutes did not show significantly different relative abundances between the sites (Table 3).

Permafrost-associated OTUs

Despite the strong phylum level differences, heterogeneity can be expected at lower taxonomic/phylogenetic levels and, in the following, we attempt to shed more light on the differences at the OTU level. The bipartite network, showing the OTU distribution among the different samples, strongly supported the observed differences in community structure (Fig. 3). Soils from the SE slope shared more OTUs than soils from the NW slope, and highest connectivity was found among the three samples originating from the same site group. More than half of the observed OTUs (2941 OTUs accounting for 16% of the abundance) were only found at the NW slope, 1233 of which were only found in the permafrost layer (Fig. 3a). In agreement with the phylum level patterns, many bacterial OTUs assigned to candidate phyla OD1, GN02, OP11 and TM7 (forming the superphylum Patescibacteria) were more abundant at the NW slope, particularly in the permafrost layer (Fig. 3b).

Indicator species analysis at the OTU level revealed a total of 1357 OTUs that were significantly ($q < 0.05$) associated with the permafrost layer and the most salient patterns will be listed in the following (Fig. 4, marked with red circled numbers no.). Most prominently, and in agreement with the pattern already observed in Fig. 3b, a majority of the permafrost-associated OTUs were affiliated with diverse (in terms of OTU richness) candidate phyla such as OD1, TM7, GN02 and OP11, or were unclassified at the domain level (Fig. 4, no. 1). In fact, with 626 OTUs, candidate OD1 was the second richest phylum at the study site (after Proteobacteria with 710 OTUs) and accounted for 28% of all bacterial sequences recovered from the permafrost. Other taxonomic groups of OTUs that were associated with the permafrost layer included abundant lichenized fungi such as the ascomycetous *Lecidea*, *Acarospora* or *Umbilicaria* (no. 2), cold-adapted yeasts such as basidiomycetous *Rhodotorula*, *Cryptococcus*, *Mrakia* or *Leucosporidium* (no. 3), Betaproteobacteria from the family Comamonadaceae such as *Polaromonas*, *Rhodoferax*, *Methylibium* or from the family Methylophilaceae and its genus *Methylotenera* (no. 4), Gammaproteobacteria from the family Coxiellaceae and its genus *Aquicella* (no. 5) or from the family Legionellaceae and its genera *Legionella* and *Tatlockia* (no. 6), Alphaproteobacteria from the family Sphingomonadaceae and its genera *Kaistobacter* and *Novosphingobium* (no. 7), Bacteroidetes from the family Chitinophagaceae and its genera *Sediminibacterium* and *Segetibacter*, from the family Flavobacteriaceae and its genus *Flavobacterium*, from the family Cryomorphaceae, and from the family Sphingobacteriaceae and its genus *Pedobacter* (no. 8), Actinobacteria from the order Actinomycetales and its genera *Cryobacterium*, *Salinibacterium* and *Aeromicrobium*, or mostly uncultured or unclassified members of the orders Gaiellales and Acidimicrobiales (no. 9), several abundant but uncultured Acidobacteria from the subdivision 6 and the order iii1–15 (no. 10), Planctomycetes and its families Pirellulaceae and Planctomycetaceae (no. 11), Verrucomicrobia with genera such as *Luteolibacter* and *Prosthecobacter* (no. 12), as well as Chlamydiae with the genera *Parachlamydia*, *Rhabdochlamydia* and *Protochlamydia* (no.13). A total of 1677 OTUs (39% of the sequences) showed no statistically significant association to any specific site group or site group combination and can be considered more or less ubiquitous at the study site. This list is not exhaustive but should rather demonstrate the high taxonomic diversity of microbial taxa found in the permafrost samples (Fig. 4).

Table 3. Differences in relative abundances and OTU counts of all detected phyla between the different slopes (SE and NW) and depths (10 and 160 cm).

Taxonomy		Relative abundance (mean ± sd)[1]				OTU counts (mean ± sd)				PERMANOVA[2]			Indicator analysis[3]
Domain	Phylum	SE10	SE160	NW10	NW160	SE10	SE160	NW10	NW160	Slope	Depth	S × D	Site(s)
Bacteria	AD3	37.88 ± 2.01	39.60 ± 1.46	2.07 ± 0.67	0.10 ± 0.03	27 ± 2	24 ± 1	9 ± 0	12 ± 3	99.5***	0.0^{ns}	0.2^{ns}	SE10+SE160
Bacteria	Proteobacteria	11.57 ± 3.97	17.74 ± 0.57	18.83 ± 1.07	22.86 ± 3.86	137 ± 18	119 ± 4	332 ± 20	454 ± 12	44.1**	29.9*	1.3^{ns}	NW10+NW160+SE160
Bacteria	Verrucomicrobia	14.77 ± 3.28	9.02 ± 0.71	17.33 ± 1.92	9.63 ± 3.93	38 ± 4	30 ± 3	109 ± 4	120 ± 7	3.7^{ns}	65.6*	1.4^{ns}	NW10+SE10
Bacteria	Acidobacteria	12.76 ± 2.31	12.58 ± 0.48	14.98 ± 0.84	5.90 ± 0.60	76 ± 4	71 ± 5	87 ± 4	69 ± 1	9.8*	42.4*	39.1*	NW10+SE10+SE160
Bacteria	OD1	0.11 ± 0.11	0.36 ± 0.16	9.56 ± 2.30	27.60 ± 7.57	10 ± 2	12 ± 2	211 ± 1	529 ± 18	62.2***	15.5*	14.6*	NW160
Bacteria	Chloroflexi	9.85 ± 0.56	7.17 ± 0.20	7.76 ± 1.59	2.70 ± 0.13	91 ± 6	85 ± 6	119 ± 5	85 ± 3	37.1**	51.4*	4.9^{ns}	NW10+SE10+SE160
Bacteria	Planctomycetes	4.42 ± 0.62	3.03 ± 0.05	5.61 ± 0.83	5.44 ± 0.52	91 ± 7	77 ± 3	145 ± 3	101 ± 10	63.1**	11.9^{ns}	7.3^{ns}	NW10+NW160+SE10
Bacteria	Actinobacteria	1.57 ± 0.39	2.56 ± 0.18	8.82 ± 2.03	3.35 ± 0.05	55 ± 7	56 ± 3	121 ± 6	131 ± 6	46.9***	14.6*	30.2*	NW10
Bacteria	Gemmatimonadetes	2.98 ± 0.67	2.44 ± 0.08	6.58 ± 0.43	2.83 ± 0.21	13 ± 1	14 ± 4	41 ± 1	37 ± 1	34.2**	39.6*	22.2*	NW10
Bacteria	Bacteroidetes	0.13 ± 0.07	0.13 ± 0.03	3.36 ± 0.55	5.88 ± 2.65	10 ± 2	5 ± 1	89 ± 5	96 ± 6	71.5**	5.6^{ns}	5.6^{ns}	NW10+NW160
Bacteria	Nitrospirae	0.68 ± 0.10	2.07 ± 0.10	1.15 ± 0.11	0.78 ± 0.12	6 ± 1	10 ± 0	8 ± 0	4 ± 1	13.4**	21.0*	63.1**	SE160
Bacteria	TM7	0.02 ± 0.01	0.01 ± 0.01	0.20 ± 0.19	3.07 ± 1.32	3 ± 1	2 ± 1	18 ± 2	130 ± 4	33.1***	25.8*	26.2*	NW160
Bacteria	GN02	0.10 ± 0.07	0.00 ± 0.00	0.56 ± 0.02	2.13 ± 0.83	2 ± 0	0 ± 0	28 ± 3	78 ± 6	49.7***	15.9*	20.7*	NW160
Bacteria	WPS-2	1.25 ± 0.11	0.68 ± 0.04	0.01 ± 0.01	0.02 ± 0.01	15 ± 2	10 ± 1	2 ± 1	5 ± 1	84.4***	7.1*	7.7**	SE10+SE160
Bacteria	Chlorobi	0.10 ± 0.02	0.11 ± 0.01	0.36 ± 0.03	0.51 ± 0.03	3 ± 1	5 ± 0	10 ± 1	8 ± 1	89.6***	5.1*	4.1*	NW10+NW160
Bacteria	Cyanobacteria	0.26 ± 0.07	0.32 ± 0.02	0.18 ± 0.04	0.23 ± 0.05	13 ± 2	8 ± 2	8 ± 1	13 ± 2	44.4*	17.5^{ns}	0.4^{ns}	none
Bacteria	OP11	0.00 ± 0.00	0.00 ± 0.00	0.02 ± 0.01	0.92 ± 0.26	0 ± 0	0 ± 0	4 ± 1	16 ± 1	32.7***	30.3*	30.3*	NW160
Bacteria	Elusimicrobia	0.06 ± 0.02	0.14 ± 0.02	0.18 ± 0.03	0.11 ± 0.01	7 ± 3	9 ± 1	12 ± 1	10 ± 2	23.7*	0.1^{ns}	62.0**	NW10+SE160
Bacteria	Chlamydiae	0.01 ± 0.00	0.01 ± 0.00	0.08 ± 0.01	0.33 ± 0.07	2 ± 1	2 ± 1	7 ± 2	28 ± 1	53.3***	22.1*	20.2*	NW160
Bacteria	WS3	0.00 ± 0.00	0.00 ± 0.00	0.15 ± 0.05	0.27 ± 0.10	0 ± 0	1 ± 1	5 ± 1	4 ± 1	73.6***	6.9^{ns}	6.5^{ns}	NW10+NW160
Bacteria	TM6	0.02 ± 0.02	0.04 ± 0.01	0.13 ± 0.01	0.21 ± 0.04	4 ± 2	5 ± 2	23 ± 3	24 ± 2	83.4***	8.9*	2.5^{ns}	NW10+NW160
Bacteria	Armatimonadetes	0.04 ± 0.03	0.00 ± 0.00	0.24 ± 0.10	0.12 ± 0.02	3 ± 1	0 ± 0	7 ± 2	6 ± 1	64.9***	14.1^{ns}	3.8^{ns}	NW10+NW160
Bacteria	OP3	0.00 ± 0.00	0.00 ± 0.00	0.21 ± 0.07	0.09 ± 0.02	0 ± 0	0 ± 1	8 ± 1	7 ± 1	68.7***	10.5*	10.7*	NW10
Bacteria	SR1	0.00 ± 0.00	0.00 ± 0.00	0.02 ± 0.00	0.20 ± 0.07	0 ± 0	0 ± 0	4 ± 2	7 ± 1	38.1***	25.5*	25.5*	NW160
Bacteria	Firmicutes	0.04 ± 0.03	0.07 ± 0.01	0.03 ± 0.02	0.04 ± 0.04	6 ± 3	7 ± 0	3 ± 3	7 ± 2	16.7^{ns}	13.2^{ns}	0.8^{ns}	none
Bacteria	MVP-21	0.00 ± 0.00	0.00 ± 0.00	0.00 ± 0.00	0.10 ± 0.02	0 ± 0	0 ± 0	1 ± 1	7 ± 1	34.2***	31.3*	31.3*	NW160
Bacteria	GAL15	0.10 ± 0.01	0.00 ± 0.00	0.00 ± 0.00	0.00 ± 0.00	1 ± 0	0 ± 0	0 ± 0	0 ± 0	33.1*	33.1*	33.1*	SE10
Bacteria	NKB19	0.00 ± 0.00	0.00 ± 0.00	0.07 ± 0.02	0.03 ± 0.03	0 ± 0	0 ± 0	2 ± 0	1 ± 1	55.3**	10.1^{ns}	10.1^{ns}	NW10
Bacteria	Fibrobacteres	0.00 ± 0.00	0.00 ± 0.00	0.03 ± 0.03	0.06 ± 0.04	0 ± 0	0 ± 0	2 ± 1	2 ± 1	48.1*	5.1^{ns}	5.1^{ns}	NW10+NW160
Bacteria	WS2	0.00 ± 0.00	0.00 ± 0.00	0.04 ± 0.02	0.03 ± 0.01	0 ± 0	0 ± 0	2 ± 1	2 ± 1	82.4**	0.4^{ns}	0.4^{ns}	NW10+NW160
Bacteria	Caldiserica	0.00 ± 0.00	0.00 ± 0.00	0.00 ± 0.00	0.06 ± 0.02	0 ± 0	0 ± 0	0 ± 0	1 ± 0	30.7*	30.7*	30.7*	NW160
Bacteria	BRC1	0.00 ± 0.00	0.00 ± 0.00	0.04 ± 0.02	0.01 ± 0.00	0 ± 0	0 ± 0	7 ± 2	3 ± 1	52.4***	17.7*	17.7*	NW10
Bacteria	FCPU426	0.01 ± 0.00	0.03 ± 0.01	0.01 ± 0.01	0.00 ± 0.00	2 ± 0	2 ± 0	2 ± 2	2 ± 1	39.3*	5.6^{ns}	29.2*	SE160
Bacteria	WS5	0.00 ± 0.00	0.00 ± 0.00	0.00 ± 0.00	0.04 ± 0.01	0 ± 0	0 ± 0	0 ± 0	1 ± 0	32.9*	32.9*	32.9*	NW160
Bacteria	Kazan-3B-28	0.00 ± 0.00	0.00 ± 0.00	0.00 ± 0.00	0.03 ± 0.00	0 ± 0	0 ± 0	1 ± 1	3 ± 0	39.4**	29.8*	29.8*	NW160
Bacteria	Thermi	0.00 ± 0.00	0.00 ± 0.00	0.00 ± 0.00	0.00 ± 0.00	0 ± 0	0 ± 0	1 ± 1	1 ± 1	30.2^{ns}	1.3^{ns}	1.3^{ns}	none
Bacteria	BHI80-139	0.00 ± 0.00	0.00 ± 0.00	0.00 ± 0.00	0.00 ± 0.00	1 ± 1	1 ± 0	0 ± 0	0 ± 0	40.1**	17.2^{ns}	17.2^{ns}	SE160
Bacteria	FBP	0.00 ± 0.00	0.00 ± 0.00	0.00 ± 0.00	0.00 ± 0.00	0 ± 0	1 ± 1	0 ± 0	0 ± 0	17.9^{ns}	17.9^{ns}	17.9^{ns}	none
Bacteria	ZB3	0.00 ± 0.00	0.00 ± 0.00	0.00 ± 0.00	0.00 ± 0.00	0 ± 0	0 ± 0	0 ± 0	1 ± 1	20.0^{ns}	20.0^{ns}	20.0^{ns}	none
Bacteria	Unclassified bacteria	0.61 ± 0.05	1.34 ± 0.18	1.06 ± 0.23	3.74 ± 1.08	19 ± 4	26 ± 2	76 ± 17	178 ± 8	30.2**	43.2*	14.2*	NW160
Archaea	Crenarchaeota	0.67 ± 0.10	0.55 ± 0.20	0.04 ± 0.01	0.00 ± 0.00	9 ± 0	6 ± 1	2 ± 1	1 ± 1	89.0**	1.6^{ns}	0.5^{ns}	SE10+SE160
Archaea	Euryarchaeota	0.01 ± 0.01	0.01 ± 0.00	0.22 ± 0.09	0.55 ± 0.21	1 ± 1	1 ± 1	5 ± 1	7 ± 1	62.0***	11.6^{ns}	10.9^{ns}	NW160

Table 3. (*Continued*).

Taxonomy		Relative abundance (mean ± sd)[1]				OTU counts (mean ± sd)				PERMANOVA[2]			Indicator analysis[3]
Domain	Phylum	SE10	SE160	NW10	NW160	SE10	SE160	NW10	NW160	Slope	Depth	S × D	Site(s)
Archaea	Parvarchaeota	0.00 ± 0.00	0.00 ± 0.00	0.06 ± 0.09	0.01 ± 0.00	0 ± 0	0 ± 0	1 ± 1	1 ± 1	17.0*	7.9^{ns}	7.9^{ns}	none
Fungi	Ascomycota	45.26 ± 5.20	36.98 ± 4.90	50.67 ±24.65	56.79 ± 6.27	70 ± 9	50 ± 6	73 ± 22	162 ± 27	23.5^{ns}	0.2^{ns}	7.6^{ns}	none
Fungi	Zygomycota	38.59 ± 2.56	35.75 ± 2.93	2.27 ± 0.94	10.77 ± 4.22	15 ± 3	11 ± 1	14 ± 7	12 ± 2	93.7***	0.8^{ns}	3.2*	SE10+SE160
Fungi	Basidiomycota	0.71 ± 0.50	2.91 ± 0.54	9.90 ± 7.95	14.88 ± 1.01	30 ± 12	24 ± 5	58 ± 24	71 ± 2	65.9**	7.6^{ns}	1.1^{ns}	none
Fungi	Chytridiomycota	0.02 ± 0.03	0.21 ± 0.08	1.37 ± 2.00	0.09 ± 0.05	1 ± 1	1 ± 0	5 ± 1	4 ± 1	9.8^{ns}	7.4^{ns}	14.0*	none
Fungi	Unclassified fungi	14.12 ± 8.63	14.03 ± 1.69	12.64 ± 5.52	13.84 ± 0.80	31 ± 13	24 ± 3	41 ± 13	53 ± 5	0.9^{ns}	0.4^{ns}	0.6^{ns}	none
Protists	Ciliophora	0.04 ± 0.05	0.01 ± 0.00	21.56 ± 29.65	2.66 ± 0.92	3 ± 1	2 ± 1	9 ± 1	10 ± 2	16.4**	9.9^{ns}	9.8^{ns}	none
Protists	Unclassified alveolata	0.00 ± 0.00	0.00 ± 0.00	0.13 ± 0.16	0.01 ± 0.01	0 ± 0	0 ± 0	1 ± 0	0 ± 1	16.3**	13.1^{ns}	13.1^{ns}	NW10
Protists	Cercozoa	0.00 ± 0.00	0.00 ± 0.00	0.05 ± 0.03	0.01 ± 0.01	0 ± 0	0 ± 0	1 ± 0	1 ± 1	31.1**	17.8^{ns}	17.8^{ns}	NW10
Green algae	Chlorophyta	1.27 ± 1.29	10.11 ± 5.17	1.41 ± 1.03	0.64 ± 0.30	4 ± 1	5 ± 1	13 ± 9	14 ± 2	26.9**	20.2*	28.6*	SE160
Green algae	Streptophyta	0.01 ±0.01	0.00 ± 0.00	0.00 ± 0.00	0.31 ± 0.04	1 ± 1	0 ± 0	1 ± 1	1 ± 0	33.3**	31.5*	33.8*	NW160

[1]Since two different targets have been used (16S rRNA for prokaryotes and ITS for eukaryotes), relative abundances are provided separately for each target and the numbers in the columns add up to 200%.
[2]Influence of slope, depth and interaction on the relative abundance of major microbial groups as determined by univariate permutational analysis of variance (PERMANOVA). Values represent the explained variance (R2) and the level of significance (***$P < 0.001$, **$P < 0.01$, *$P < 0.05$, ^{ns}not significant). *P*-values were adjusted for multiple comparisons using the Benjamini–Hochberg correction.
[3]Site (i.e. SE10, SE160, NW10 and NW160) or site combination to which the phylum was significantly associated as determined by correlation-based indicator species analysis. *P*-values were adjusted for multiple comparisons using the Benjamini–Hochberg correction.

DISCUSSION

Most of our current knowledge on molecular microbial diversity of permafrost habitats is based on polar regions, whereas high-throughput sequencing surveys in temperate mountain permafrost areas are largely missing, despite the fact that altitudinal permafrost sites are fundamentally different from latitudinal permafrost sites (Margesin 2009). At higher altitudes, e.g. the Alps, microclimatic factors, such as high temperature fluctuations, freeze–thaw cycles and UV radiation can have a large impact on soil microbial communities (Lipson 2007; Zumsteg *et al.* 2013), in particular where the number of daily sunlight hours might differ greatly from one site to another due to their exposition to the sun. This study applied a unique sampling design in order to elucidate the microbial diversity hidden in alpine permafrost found at the long-term study site of 'Muot da Barba Peider' in SE Switzerland (Fig. S1a, Supporting Information). Sampling the cold north-facing (NW) and warm south-facing (SE) slopes of the mountain ridge, we were not only able to compare the soil microbial communities found below the permafrost table with the overlaying active layer, as it is usually reported in polar ecosystems, but also to compare the permafrost microbiota to the communities found in soils of the same depth from the adjacent SE slope experiencing seasonal freezing and thawing. This is an important aspect because comparing soils at the same depth reduces the confounding influence of external factors such as vegetation and climate that would co-determine the differences in microbial communities between the deeper permafrost layer and the overlaying active horizon.

Microbial community structures between the NW and SE slopes differed strongly, both in α- and β-diversity (Fig. 1). These differences were strongly driven by the differences in soil physico-chemical properties, which might largely be attributed to differences in weathering and biotic activity. Soil physico-chemical properties also differed along the soil profile, shaping microbial community structure. However, in contrast to the physico-chemical properties, differences in community structure between the upper and lower soil layer was much more pronounced in the NW than SE, likely caused by the presence of the permafrost table. The permafrost table is the upper boundary of the continuously frozen horizon and acts as a physical and biogeochemical barrier that limits infiltration of both surface water and external environmental factors (Steven *et al.* 2006). This barrier likely prevented any vertical movement of microbial species, but even if such events would occur, it significantly reduces the probability of contamination through 'modern' microorganisms (Kochkina *et al.* 2012) and suggests that the microorganisms that we have detected in the permafrost layer have been residing there for a long time. The ^{14}C data indicates that the deeper layers at both slopes have a similar carbon turnover, suggesting that microbial activity is similar at both sites and, thus, differences in microbial community structure might rather arise due to different permeability and altered vertical movements of the species rather than through the influence of different microbial activities and community development.

Life in permafrost soil is constrained by many factors including low temperature, oxygen limitation, osmotic and hydrostatic pressure, oxidative stress and nutrient availability (D'Amico *et al.* 2006). Due to these extreme conditions, biodiversity is expected to be low and largely consist of microbial species with structural and functional adaptations to survive or even thrive under these circumstances (D'Amico *et al.* 2006; Buzzini *et al.* 2012; Jansson and Tas 2014). The permafrost soil at this site was characterized by an unexpectedly high microbial diversity

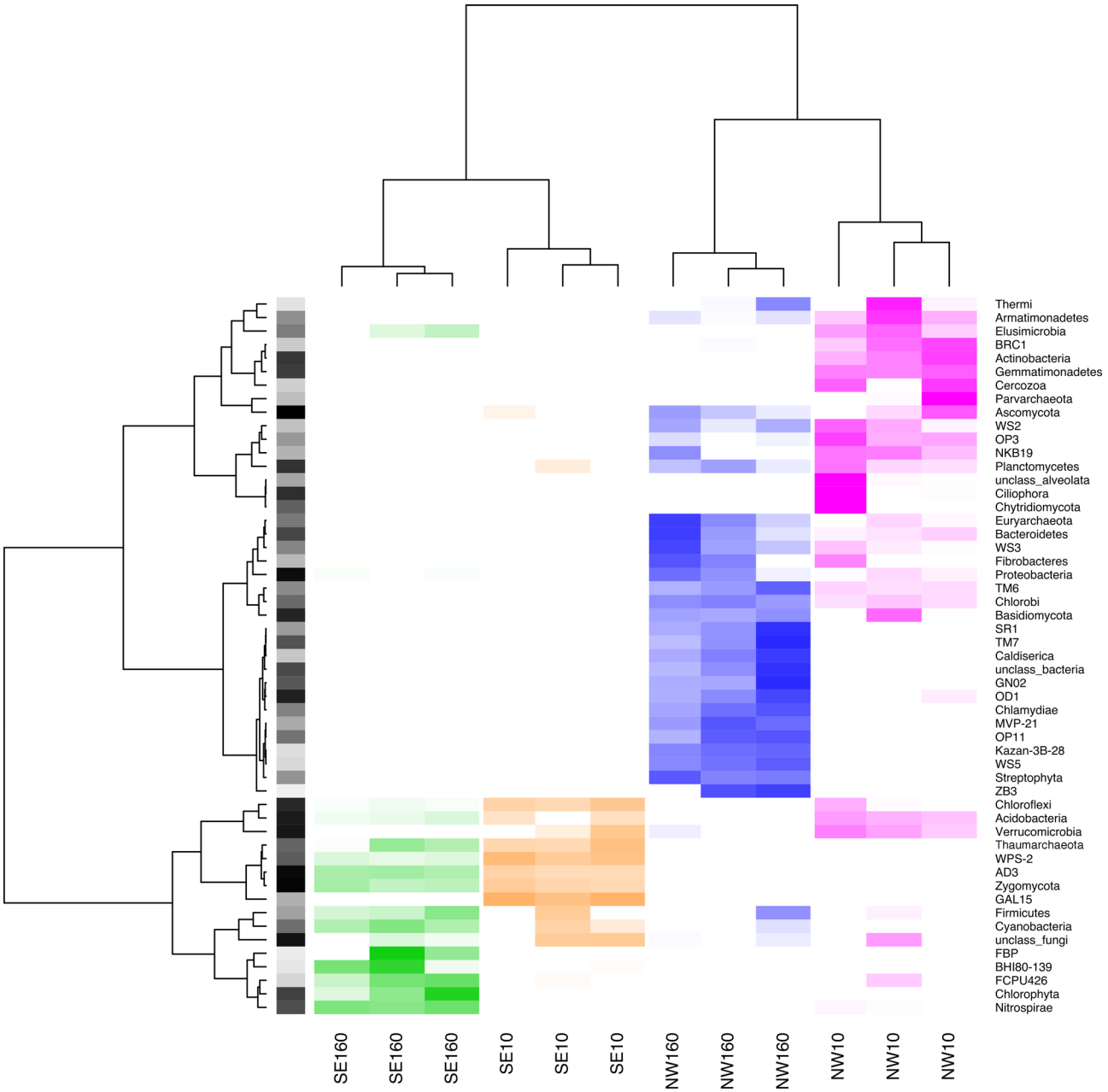

Figure 2. Heatmaps showing changes in relative abundance of phyla compared to the overall mean. Data were scaled (z-transformed) in order to compare groups of different abundances. Cluster analysis based on the Ward method was performed to group samples with similar community structure and phyla with similar sample structure. The grey heatmap represents the relative abundance of the individual phyla from low (light grey) to high abundance (black).

comprising a substantial fraction of undercharacterized microbial taxa (Figs 1–4; Table 3). The high-throughput sequencing approach of prokaryotic and eukaryotic ribosomal markers identified many OTUs of several candidate phyla with no close cultured relatives. These candidate divisions represented a substantial fraction of the microbiota at this site and might therefore play an important role in primary succession and nutrient turnover after thawing. The most prominent finding of the presented study was that the permafrost samples were significantly enriched with members of the bacterial candidate phyla OD1 (Parcubacteria), TM7 (Saccharibacteria), GN02 (Gracilibacteria) and OP11 (Microgenomates), phyla that have recently been proposed to form a new superphylum called Patescibacteria (Rinke *et al.* 2013; Sekiguchi *et al.* 2015; Shipunov 2015). Based on genomic features recovered from single-cell whole-genome sequencing, Patescibacteria (Rinke *et al.* 2013) and other related candidate phyla of the recently proposed CPR supergroup (Brown *et al.* 2015) are characterized by small genomes (approximately 1MB) with lower GC contents (30–50%) and reduced metabolic capabilities that likely have prevented their cultivation so far (Kantor *et al* 2013; Rinke *et al.* 2013; Brown *et al.* 2015). These phyla have often been recovered from anoxic environments (Peura *et al.* 2012; Ganzert, Bajerski and Wagner 2014) and metagenomic features suggest a strictly anaerobic fermentation-based lifestyle with involvement in hydrogen production and sulphur cycling (Wrighton *et al.* 2012; Wrighton *et al.*

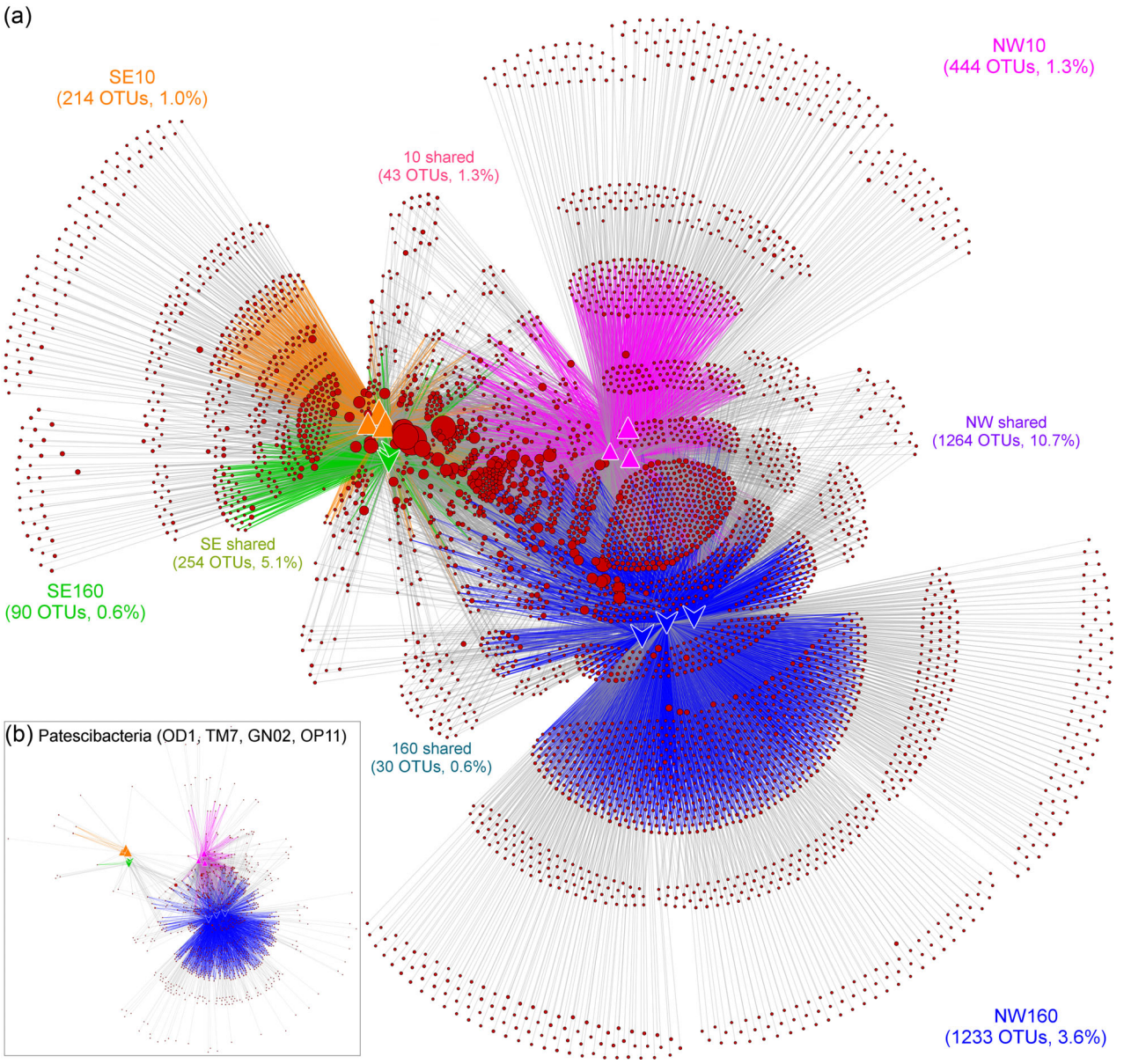

Figure 3. Bipartite network showing the OTU distribution (circles) across the different samples (triangles). Node sizes are scaled by read counts (square root). Edges connect OTUs and samples, if a particular OTU was observed in a particular sample. The edge-weighted (weighted by OTU abundance) 'Allegro Fruchterman–Reingold' algorithm applied to the network clusters samples with higher connectivity (=similar community structure). Coloured edges represent significant ($q < 0.05$) associations between OTU and the respective site group (SE10, SE160, NW10 and NW160) as determined by indicator species analysis (e.g. an OTU can be associated with a combination of site groups and have two or more coloured edges); grey edges represent non-significant associations. The number of OTUs per site group or site group combinations including their contribution to the total abundance (%) is provided in the graph. Panel (**a**) shows the bipartite network with all observed OTUs, whereas panel (**b**) shows only the OTUs assigned to the superphylum Patescibacteria including the four candidate phyla OD1 (626 OTUs), TM7 (149), GN02 (92) and OP11 (17).

2014), and, possibly, in anaerobic methane oxidation (Peura *et al.* 2012). Since permafrost environments are likely oxygen limited, these characteristics might give these organisms some selective advantages to thrive under these conditions. Small genome sizes and anaerobic lifestyles appear to be key for the survival and adaptation of micro-organisms in alpine permafrost soils, since also other candidate phyla detected at the NW slope of the study site such as WS3 (Latescibacteria) and SR1 might likely possess small genomes and anaerobic fermentative modes of metabolism (Kantor *et al.* 2013; Camanocha and Dewhirst 2014; Youssef *et al.* 2015). For example, it has been suggested that Latescibacteria might mediate the turnover of complex organic polymers of algal origin in anoxic environments (Youssef *et al.* 2015), a strategy that could help to acquire nutrients from green algae locked up in permafrost.

Among all these candidate phyla, OD1 (Parcubacteria) was standing out as being highly abundant and diverse in the permafrost samples (Figs 1 and 4). In fact, a recent study revisiting bacterial phylogeny based on 16S rRNA sequences concluded that OD1 itself might form a diverse superphylum comprising around 28 phyla (Yarza *et al.* 2014). Recent inspections of OD1 genomes highlighted the unusual biology of these organisms including absence or substantial reduction in gene sets for biosynthesis of cofactors, amino acids, nucleotides,

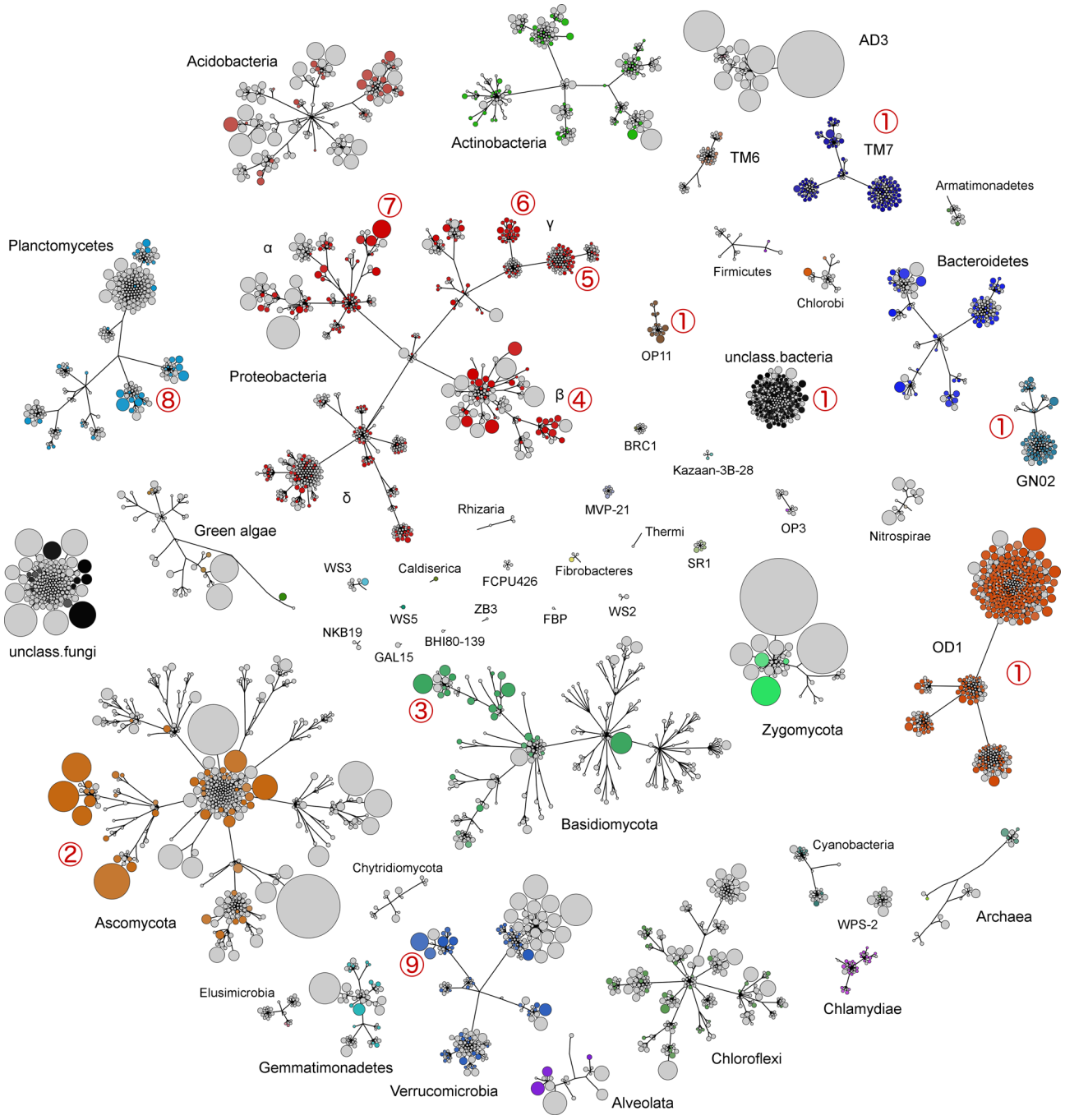

Figure 4. Taxonomic networks of the detected prokaryotic and eukaryotic communities showing the OTU distribution across the different taxonomic groups (phylum or other eukaryotic supergroups of no official rank). Nodes correspond to OTUs and node sizes correspond to their relative abundances (square root) in the data set. Edges represent the taxonomic path from the phylum to OTU level and OTUs were placed at the level of the lowest possible assignment. Coloured nodes represent OTUs that were significantly ($q < 0.05$) associated with the permafrost layer (NW160). Red circled numbers point to clusters discussed in the text.

vitamins and lipids, as well as other activities conserved in almost all other known bacterial genomes (Nelson and Stegen 2015). At the same time, OD1 members have a limited number of transport systems, indicating a sparse and unusual mechanism for nutrient and energy acquisition (Kantor *et al.* 2013; Nelson and Stegen 2015). Based on the high genotypic diversity, an observation that is supported by the high number of different OTUs detected in our study, Nelson and Stegen (2015) suggested that OD1 organisms are adapted to a wide range of growth environments and feature a high degree of specialization. Small genomes are commonly found in either free-living organisms with streamlined lifestyle to efficiently perform a limited range of metabolic activities or symbiotic organisms under metabolic dependency on the host. The lack of biosynthetic capabilities and DNA repair mechanisms as well as the presence of an array of potential attachment and adhesion proteins might indicate that Parcubacteria are broad-range ectosymbionts or parasites attached to the surface of other microbial cells to gain access to nutrient and energy sources acquired by the host cells. Such a mutualistic, commensal or parasitic lifestyle could be one

successful strategy to gain advantage in the limited permafrost environment.

Previous high-throughput sequencing studies show an equivocal picture of the relative abundance of Patescibacteria-like candidate divisions in permafrost environments. In general, these phyla were detected at comparatively low abundance or absent from the libraries (Yang *et al.* 2012; Frank-Fahle *et al.* 2014; Gittel *et al.* 2014; Tas *et al.* 2014; Vishnivetskaya *et al.* 2014; Jiang *et al.* 2015); however, we are not aware of any comparable report on alpine permafrost. It is not yet clear, if these discrepancies solely arise from large differences in community composition across different permafrost habitats as reviewed recently (Jansson and Tas 2014) or are also influenced by methodological differences across studies including DNA extraction (Vishnivetskaya *et al.* 2014), primer specificities and downstream analysis such taxonomic classification. Therefore, it is too early to conclude on the universality of these findings, as few high-throughput sequencing studies have surveyed microbial communities in permafrost and, to the best of our knowledge, none in European alpine habitats. The occurrence of many undercharacterized candidate phyla with no cultured representatives, in particular OD1, in the permafrost soils at 'Muot da Barba Peider' is unprecedented and highlights our poor understanding of the biology in these habitats and the microbial metabolisms required to adapt to such extreme conditions. After all, the distinct metabolism of these uncultured divisions and their unique strategies to adapt to more extreme habitats might be more common than previously expected (Rinke *et al.* 2013; Brown *et al.* 2015).

Not all candidate phyla were associated with the NW flank of the ridge. Candidate phylum AD3, the most abundant phylum in this dataset, as well as WPS-2 and GAL15 were more abundant at the SE slope. It has been shown previously that AD3 are abundant members in the active layer of permafrost-like habitats (Tas *et al.* 2014; Schostag *et al.* 2015) and thrive in soils of low carbon contents (Jansson and Tas 2014). The predominance of AD3 at the SE slope suggests a successful adaptation to the harsh conditions of seasonal freeze-thaw cycles and strong UV radiation.

Among better-established bacterial phyla, Proteobacteria, Verrucomicrobia, Acidobacteria, Chloroflexi, Planctomycetes, Actinobacteria, Gemmatimonadetes, Bacteroidetes and Nitrospirae were abundant at 'Muot da Barba Peider' (Table 3). Surprisingly, only very few Firmicutes were detected (0.04%), although it has been suggested that these spore-forming species might be well adapted to cold conditions and have frequently been discovered in permafrost-like habitats (Hultman *et al.* 2015). Bacteroidetes is another phylum that has frequently been associated with permafrost soils (Mackelprang *et al.* 2011). In the present study, Bacteroidetes were significantly more abundant at the NW slope with a tendency to increased abundance in the permafrost layer. We found permafrost-associated OTUs among the families Chitinophagaceae, Flavobacteriaceae, Cryomorphaceae and Sphingobacteriaceae, observations that were similar to previous reports in a recent high-throughput sequencing study of permafrost habitats in Greenland (Ganzert, Bajerski and Wagner 2014). Reportedly, members of these families are often psychrotolerant and capable of degrading biopolymers such as chitin or plant-derived polymers. Other major phyla commonly observed in permafrost such as Chloroflexi, Acidobacteria and Actinobacteria appeared to thrive better outside the permafrost, but it has recently been reviewed that the relative abundance of these phyla in permafrost can greatly vary among different geographical locations (Jansson and Tas 2014) and cold-adaptive members of these diverse and globally ubiquitous bacterial phyla might rather have to be identified at lower phylogenetic levels (Fig. 4).

Archaea comprised only around 0.5% of the relative abundance, which is in agreement with previous reports in cold permafrost-like habitats (Wilhelm *et al.* 2011; Tveit *et al.* 2013). It remains an open question, if this result represents reality or just another amplification bias of this relatively understudied domain of life. Although the newly modified primers have been tailored *in silico* to improve detection of archaeal 16S rRNA signatures, they still lack near-full coverage of the archaeal domain. Nevertheless, we found a clear difference in archaeal community composition between the SE and NW slope. Whereas Thaumarchaeota were more abundant at the SE slope, Euryarchaeota appeared to be better adapted to the NW (Table 3). All nine euryarchaeal OTUs were assigned to the order E2 of the class Thermoplasmata. This seems surprising as Thermoplasmata are common acidophilic thermophiles, but members assigned to this class have already previously been detected in permafrost soils (Karaevskaya *et al.* 2014; Jiang *et al.* 2015), likely because of their adaptation to anaerobic conditions (Lin *et al.* 2015).

We also found an impressive diversity of fungi at the study site. A total of 840 fungal OTUs accounted for 93% of the detected eukaryotic sequences with Ascomycota (46%) being much more abundant than Zygomycota (27%) and Basidiomycota (7%), which is largely in agreement with previous high-throughput sequencing surveys in permafrost (Zhang *et al.* 2013; Jiang *et al.* 2015). Notably, 14% of the fungal sequences could not be assigned beyond kingdom level, indicating another undercharacterized microbial fraction in these extreme environments. The fungal community in the permafrost layer was characterized by abundant yeasts and lichenized fungi (Fig. 4). These fungal groups are common in cryosphere environments because they have developed successful structural and functional adaptations (e.g. spore formation, membrane modification, production of cryoprotectants and synthesis of enzymes operating at low temperatures) not only to survive but also to be metabolically active and propagate under extremely cold and nutrient poor conditions (Ozerskaya *et al.* 2009; Buzzini *et al.* 2012; Buzzini and Margesin 2014). Therefore, it was not surprising that we recovered many of the fungal genera commonly found in permafrost-like habitats (Margesin and Miteva 2011; Zalar and Gunde-Cimerman 2014), including yeasts such as *Rhodotorula*, *Cryptococcus*, *Mrakia* and *Leucosporidium*, as well as lichenized fungi such as *Lecidea*, *Acarospora* and *Umbilicaria*. Although it has been shown that lichens can maintain photosynthetic activity at sub-zero temperatures, e.g. down to –17°C (Lydolph *et al.* 2005), it is unlikely that they are photosynthetically active in sediment permafrost at a depth of 1.6 m and their potential photobionts (green algae and cyanobacteria), were only detected at a much lower relative abundance. These facultative symbionts rather occur as free-living fungi surviving at low levels of nutrients and it has been shown that lichenizing fungi survive in deep dark permafrost in resting states and are readily reversible to proliferation with the capability for photosynthesis after thawing (Vishnivetskaya 2009). Reduction of metabolic rates and nutrient uptake as well as storage of carbon and energy in various forms (e.g. glycogen, polyhydroxyalkanoates, polyphosphates, triglycerides and wax esters) is one important feature of cold-adapted microorganisms (Jansson and Tas 2014) and might equally apply to the abundant fungi and bacteria found in the permafrost samples at 'Muot da Barba Peider'.

The extent of microbial α-diversity recovered from the permafrost layer was astonishing and significantly exceeded the diversity in the surrounding active soils (Fig. 1). It needs to be

clarified, however, that diversity has been standardized by number of sequences, which might not be the same as the total diversity at the sites, since the permafrost samples contained around ten times less DNA than the corresponding deeper SE layer and around 100–300 times less DNA than the overlaying active layer at both slopes. Nevertheless, alpine permafrost soils appear to be a rich genetic resources consisting of multiple phylogenetic clades. Although a significant proportion of the sequenced DNA might originate from dead or dormant cells or even from remains of persisting extracellular DNA, and the sequencing approach cannot distinguish between viable and dead cells, several recent studies have demonstrated significant microbial activity in permafrost soils at ambient sub-zero temperatures (Steven *et al*. 2008; Margesin 2009; Buzzini and Margesin 2014). Therefore, some of these cells have the potential to propagate and spread once released into the environment after thawing with potential consequences for ecosystem development.

CONCLUSION

The present study illustrates that high alpine permafrost soil may harbour a diverse and largely undercharacterized microbiome. More comprehensive studies investigating altitudinal permafrost in temperate mountain regions are required to confirm the universality of the findings as well as to unravel the metabolic potential locked up in these environments. Our findings suggest that alpine permafrost habitats are not as inhospitable as previously appreciated, but give rise to an immense diversity of microbial species with unique structural and functional adaptation mechanisms required for survival and even propagation under low temperatures, limited water and oxygen availability and poor nutrient levels. In particular, members of the bacterial candidate superphylum Patescibacteria, suggestively featuring small streamlined genomes, reduced anaerobic metabolisms and potential ectosymbiotic lifestyles, as well as cold-adapted yeast-like and lichenized fungi appear to be characteristic for these environments. The development of targeted cultivation methods and/or application of techniques such as stable isotope probing will ultimately allow identifying viable and metabolically active microorganisms. Recent advances in DNA sequencing technologies offer an unprecedented opportunity to characterize and better understand the unique soil microbiome hidden in permafrost and to elucidate their dependency on environmental factors at the larger scale. Cutting-edge techniques such as single-cell genomics might now provide much deeper insights into the peculiar metabolisms of these uncultivated and poorly characterized permafrost inhabitants. With the accelerated thawing of permafrost soils in temperate alpine mountains, it becomes increasingly important to understand the biological dynamics of these environments in order to anticipate potential ecological trajectories in a warming world.

SUPPLEMENTARY DATA

Supplementary data are available at FEMSEC online.

ACKNOWLEDGEMENTS

We gratefully thank the Central Laboratory and Roger Koechli (Swiss Federal Research Institute WSL) for completing chemical analyses and providing help in the laboratory. The authors also thank the Genetic Diversity Center (GDC) at ETH Zürich and acknowledge the contribution of scientists at the McGill University and Génome Québec Innovation Center, Montréal, Canada, for the paired-end sequencing on Illumina MiSeq.

FUNDING

This study was funded by the internal WSL project (PSP 5233.00029.002.01), the Swiss National Science Foundation (SNSF) under the grant number 31003A-138321 and the Agroscope Research Program 'Microbial Biodiversity'.

Conflict of interest. None declared.

REFERENCES

Abarenkov K, Nilsson RH, Larsson KH *et al*. The UNITE database for molecular identification of fungi—recent updates and future perspectives. *New Phytol* 2010;**186**:281–5.

Anderson MJ. A new method for non-parametric multivariate analysis of variance. *Aust J Ecol* 2001;**26**:32–46.

Anderson MJ. Distance-based tests for homogeneity of multivariate dispersions. *Biometrics* 2006;**62**:245–53.

Bengtsson-Palme J, Hartmann M, Eriksson KM *et al*. Metaxa2: improved identification and taxonomic classification of small and large subunit rRNA in metagenomic data. *Mol Ecol Resour* 2015;**15**:1403–14.

Bengtsson-Palme J, Ryberg M, Hartmann M *et al*. Improved software detection and extraction of ITS1 and ITS2 from ribosomal ITS sequences of fungi and other eukaryotes for analysis of environmental sequencing data. *Methods Ecol Evol* 2013;**4**:914–9.

Benjamini Y, Hochberg Y. Controlling the false discovery rate: a practical and powerful approach to multiple testing. *J Roy Stat Soc B* 1995;**57**:289–300.

Benson DA, Clark K, Karsch-Mizrachi I *et al*. GenBank. *Nucleic Acids Res* 2015;**43**:D30–5.

Brown CT, Hug LA, Thomas BC *et al*. Unusual biology across a group comprising more than 15% of domain Bacteria. *Nature* 2015;**523**:208–11.

Buzzini P, Branda E, Goretti M *et al*. Psychrophilic yeasts from worldwide glacial habitats: diversity, adaptation strategies and biotechnological potential. *FEMS Microbiol Ecol* 2012;**82**:217–41.

Buzzini P, Margesin R. *Cold-Adapted Yeasts—Biodiversity, Adaptation Strategies and Biotechnological Significance*. Heidelberg, Germany: Springer, 2014.

Camanocha A, Dewhirst FE. Host-associated bacterial taxa from chlorobi, chloroflexi, Gn02, synergistetes, SR1, TM7, and WPS-2 Phyla/candidate divisions. *J Oral Microbiol* 2014;**6**:25468.

Clarke KR. Non-parametric multivariate analyses of changes in community structure. *Aust J Ecol* 1993;**18**:117–43.

Clarke KR, Gorley RN. *PRIMER v6: User Manual/Tutorial*. PRIMER-E; Plymouth, 2006.

D'Amico S, Collins T, Marx JC *et al*. Psychrophilic microorganisms: challenges for life. *EMBO Rep* 2006;**7**:385–9.

De Cáceres M, Legendre P. Associations between species and groups of sites: indices and statistical inference. *Ecology* 2009;**90**:3566–74.

De Cáceres M, Legendre P, Moretti M. Improving indicator species analysis by combining groups of sites. *Oikos* 2010;**119**:1674–84.

DeConto RM, Galeotti S, Pagani M *et al*. Past extreme warming events linked to massive carbon release from thawing permafrost. *Nature* 2012;**484**:87–91.

DeSantis T, Hugenholtz P, Larsen N *et al*. Greengenes, a chimera-checked 16S rRNA gene database and workbench compatible with ARB. *Appl Environ Microbiol* 2006;**72**:5069–72.

Edgar R. Search and clustering orders of magnitude faster than BLAST. *Bioinformatics*. 2010;**26**:2460–1.

Edgar R, Haas B, Clemente J *et al*. UCHIME improves sensitivity and speed of chimera detection. *Bioinformatics* 2011;**27**:2194–2200.

Edgar RC. UPARSE: highly accurate OTU sequences from microbial amplicon reads. *Nat Methods* 2013;**10**:996–8.

Edgar RC, Flyvbjerg H. Error filtering, pair assembly, and error correction for next-generation sequencing reads. *Bioinformatics* 2015;**31**:3476–82.

Fox J, Weisberg S. *An R Companion to Applied Regression, Second Edition*. Thousand Oaks, CA: SAGE, 2011.

Frank-Fahle BA, É Yergeau, Greer CW *et al*. Microbial functional potential and community composition in permafrost-affected soils of the NW Canadian Arctic. *PLoS One* 2014;**9**:e84761.

Fruchterman TMJ, Reingold EM. Graph drawing by force-directed placement. *Software Pract Exper* 1991;**21**:1129–64.

Ganzert L, Bajerski F, Wagner D. Bacterial community composition and diversity of five different permafrost-affected soils of Northeast Greenland. *FEMS Microbiol Ecol* 2014;**89**:426–41.

Gee G, Bauder J. *Texture, Hydrometer Method*. Soil Science Scociety of America: Madison, WI, USA, 1986.

Gittel A, Bárta J, Kohoutová I *et al*. Site- and horizon-specific patterns of microbial community structure and enzyme activities in permafrost-affected soils of Greenland. *Front Microbiol* 2014;**5**:541.

Gower JC. Some distance properties of latent root and vector methods used in multivariate analysis. *Biometrika* 1966;**53**:325–38.

Graham DE, Wallenstein MD, Vishnivetskaya TA *et al*. Microbes in thawing permafrost: the unknown variable in the climate change equation. *ISME J* 2012;**6**:709–12.

Haeberli W, Gruber S. Global warming and mountain permafrost. In: Margesin R (ed.). *Permafrost Soils*. Heidelberg, Germany: Springer, 2009, 205–18.

Hajdas I. Radiocarbon dating and its applications in Quaternary studies. *Eiszeitalter und Gegen Quat Sci J* 2008;**57**:24.

Hartmann M, Frey B, Mayer J *et al*. Distinct soil microbial diversity under long-term organic and conventional farming. *ISME J* 2015;**9**:1177–94.

Hartmann M, Niklaus PA, Zimmermann S *et al*. Resistance and resilience of the forest soil microbiome to logging-associated compaction. *ISME J* 2014;**8**:226–44.

Hollesen J, Elberling B, Jansson PE. Future active layer dynamics and carbon dioxide production from thawing permafrost layers in Northeast Greenland. *Glob Change Biol* 2011;**17**:911–26.

Hultman J, Waldrop MP, Mackelprang R *et al*. Multi-omics of permafrost, active layer and thermokarst bog soil microbiomes. *Nature* 2015;**521**:208–12.

Huss M. Present and future contribution of glacier storage change to runoff from macroscale drainage basins in Europe. *Water Resour Res* 2011;**47**:W07511.

Jansson JK, Tas N. The microbial ecology of permafrost. *Nat Rev Microbiol* 2014;**12**:414–25.

Jiang N, Li Y, Zheng C *et al*. Characteristic microbial communities in the continuous permafrost beside the bitumen in Qinghai-Tibetan Plateau. *Environ Earth Sci* 2015;**74**:1343–52.

Käll L, Storey JD, Noble WS. qvality: non-parametric estimation of q-values and posterior error probabilities. *Bioinformatics* 2009;**25**:964–6.

Kantor RS, Wrighton KC, Handley KM *et al*. Small genomes and sparse metabolisms of sediment-associated bacteria from four candidate phyla. *mBio* 2013;**4**:e00708–00713.

Karaevskaya ES, Demchenko LS, Demidov NE *et al*. Archaeal diversity in permafrost deposits of Bunger Hills Oasis and King George Island (Antarctica) according to the 16S rRNA gene sequencing. *Microbiology* 2014;**83**:398–406.

Kochkina G, Ivanushkina N, Ozerskaya S *et al*. Ancient fungi in Antarctic permafrost environments. *FEMS Microbiol Ecol* 2012;**82**:501–9.

Koven CD, Ringeval B, Friedlingstein P *et al*. Permafrost carbon-climate feedbacks accelerate global warming. *P Natl Acad Sci USA* 2011;**108**:14769–74.

Legendre M, Bartoli J, Shmakova L *et al*. Thirty-thousand-year-old distant relative of giant icosahedral DNA viruses with a pandoravirus morphology. *Proc Natl Acad Sci USA* 2014;**111**:4274–9.

Lin X, Handley KM, Gilbert JA *et al*. Metabolic potential of fatty acid oxidation and anaerobic respiration by abundant members of Thaumarchaeota and Thermoplasmata in deep anoxic peat. *ISME J* 2015;**9**:2740–4.

Lipson DA. Relationships between temperature responses and bacterial community structure along seasonal and altitudinal gradients. *FEMS Microbiol Ecol* 2007;**59**:418–27.

Lydolph MC, Jacobsen J, Arctander P *et al*. Beringian Paleoecology inferred from permafrost-preserved fungal DNA. *Appl Environ Microbiol* 2005;**71**:1012–7.

McArdle BH, Anderson MJ. Fitting multivariate models to community data: a comment on distance-based redundancy analysis. *Ecology* 2001;**82**:290–7.

McDonald D, Price MN, Goodrich J *et al*. An improved Greengenes taxonomy with explicit ranks for ecological and evolutionary analyses of bacteria and archaea. *ISME J* 2011;**6**:610–8.

Mackelprang R, Waldrop MP, DeAngelis KM *et al*. Metagenomic analysis of a permafrost microbial community reveals a rapid response to thaw. *Nature* 2011;**480**:368–71.

Margesin R. *Permafrost Soils*. Heidelberg, Germany: Springer, 2009.

Margesin R, Feller G. Biotechnological applications of psychrophiles. *Environ Technol* 2010;**31**:835–44.

Margesin R, Miteva V. Diversity and ecology of psychrophilic microorganisms. *Res Microbiol* 2011;**162**:346–61.

Margesin R, Schinner F, Marx J-C *et al*. *Psychrophiles: From Biodiversity to Biotechnolgy*. Heidelberg, Germany: Springer, 2008.

Martin M. Cutadapt removes adapter sequences from high-throughput sequencing reads. *EMBnet J* 2011;**17**:10–12.

Nelson WC, Stegen JC. The reduced genomes of Parcubacteria (OD1) contain signatures of a symbiotic lifestyle. *Front Microbiol* 2015;**6**:713.

Nikolenko S, Korobeynikov A, Alekseyev M. BayesHammer: Bayesian clustering for error correction in single-cell sequencing. *BMC Genomics* 2013;**14**:S7.

Nilsson RH, Tedersoo L, Ryberg M *et al*. A comprehensive, automatically updated fungal ITS sequence dataset for reference-based chimera control in environmental sequencing efforts. *Microbes Environ* 2015;**30**:145–50.

Oksanen J, Blanchet FG, Kindt R *et al*. *Vegan: Community Ecology Package (V2.3-3)*. R package version 2016, 1–17.

Ozerskaya S, Kochkina G, Ivanushkina N *et al.* Fungi in permafrost. In: Margesin R (ed.). *Permafrost Soils*, Vol. **16.** Heidelberg, Germany: Springer, 2009, 85–96.

Petrova MA, Gorlenko ZM, Soina VS *et al.* Association of the strA-strB genes with plasmids and transposons in the present-day bacteria and in bacterial strains from permafrost. *Russ J Genet* 2008;**44**:1116–20.

Peura S, Eiler A, Bertilsson S *et al.* Distinct and diverse anaerobic bacterial communities in boreal lakes dominated by candidate division OD1. *ISME J* 2012;**6**:1640–52.

Phillips M, Margreth S, Ammann W. Creep of snow-supporting structures in alpine permafrost. In: Phillips M, Springman SM, Arenson LU (eds). *Proceedings of the Eighth International Conference on Permafrost*. Lisse: Balkema, 2003, 891–6.

R Core Team. *R: A language and environment for statistical computing*. R Foundation for Statistical Computing. Vienna, Austria, 2014, http://www.R-project.org/ (18 February 2016, date last accessed).

R Studio Team. *RStudio: Integrated Development for R*. Boston, MA: RStudio, Inc., 2014, https://www.rstudio.com (18 February 2016, date last accessed).

Rappe MS, Giovannoni SJ. The uncultured microbial majority. *Annu Rev Microbiol* 2003;**57**:369–94.

Reimer PJ, Bard E, Bayliss A *et al.* IntCal13 and Marine13 radiocarbon age calibration curves 0–50,000 years cal BP. *Radiocarbon* 2013;**55**:1869–87.

Rinke C, Schwientek P, Sczyrba A *et al.* Insights into the phylogeny and coding potential of microbial dark matter. *Nature* 2013;**499**:431–7.

Rist A, Phillips M. First results of investigations on hydrothermal processes within the active layer above alpine permafrost in steep terrain. *Nor J Geogr* 2005;**59**:177–83.

Schloss PD, Westcott SL, Ryabin T *et al.* Introducing mothur: open-source, platform-independent, community-supported software for describing and comparing microbial communities. *Appl Environ Microbiol* 2009;**75**:7537–41.

Schostag M, Stibal M, Jacobsen CS *et al.* Distinct summer and winter bacterial communities in the active layer of Svalbard permafrost revealed by DNA- and RNA-based analyses. *Front Microbiol* 2015;**6**:399.

Schuur EAG, Bockheim J, Canadell JG *et al.* Vulnerability of permafrost carbon to climate change: implications for the global carbon cycle. *Bioscience* 2008;**58**:701–14.

Schuur EAG, Vogel JG, Crummer KG *et al.* The effect of permafrost thaw on old carbon release and net carbon exchange from tundra. *Nature* 2009;**459**:556–9.

Sekiguchi Y, Ohashi A, Parks DH *et al.* First genomic insights into members of a candidate bacterial phylum responsible for wastewater bulking. *PeerJ* 2015;**3**:e740.

Shannon P, Markiel A, Ozier O *et al.* Cytoscape: a software environment for integrated models of biomolecular interaction networks. *Genome Res* 2003;**13**:2498–504.

Shipunov AB. *Systema Naturae v.6.11*, 2015, 17, http://ashipunov.info/shipunov/os/os-en.htm (18 February 2016, date last accessed).

Steven B, Léveillé R, Pollard W *et al.* Microbial ecology and biodiversity in permafrost. *Extremophiles* 2006;**10**:259–67.

Steven B, Pollard WH, Greer CW *et al.* Microbial diversity and activity through a permafrost/ground ice core profile from the Canadian high Arctic. *Environ Microbiol* 2008;**10**:3388–403.

Storey JD. A direct approach to false discovery rates. *J Roy Stat Soc B* 2002;**64**:479–98.

Tas N, Prestat E, McFarland JW *et al.* Impact of fire on active layer and permafrost microbial communities and metagenomes in an upland Alaskan boreal forest. *ISME J* 2014;**8**:1904–19.

Tedersoo L, Bahram M, Põlme S *et al.* Global diversity and geography of soil fungi. *Science* 2014;**346**:1256688.

Tveit A, Schwacke R, Svenning MM *et al.* Organic carbon transformations in high-Arctic peat soils: key functions and microorganisms. *ISME J* 2013;**7**:299–311.

Vishnivetskaya TA. Viable cyanobacteria and green algae from the permafrost darkness. In: Margesin R (ed.). *Permafrost Soils*, Vol. **16.** Heidelberg, Germany: Springer 2009, 73–84.

Vishnivetskaya TA, Layton AC, Lau MCY *et al.* Commercial DNA extraction kits impact observed microbial community composition in permafrost samples. *FEMS Microbiol Ecol* 2014;**87**:217–30.

Wacker L, Němec M, Bourquin J. A revolutionary graphitisation system: fully automated, compact and simple. *Nucl Instrum Meth B* 2010;**268**:931–4.

Wagner D, Gattinger A, Embacher A *et al.* Methanogenic activity and biomass in Holocene permafrost deposits of the Lena Delta, Siberian Arctic and its implication for the global methane budget. *Glob Change Biol* 2007;**13**:1089–99.

Wang Q, Garrity GM, Tiedje JM *et al.* Naive Bayesian classifier for rapid assignment of rRNA sequences into the new bacterial taxonomy. *Appl Environ Microbiol* 2007;**73**:5261–7.

Warnes GR, Bolker B, Bonebakker L *et al. Gplots: Various r Programming Tools for Plotting Data. 2013*. R package version, 2014, **2**.

Wilhelm RC, Niederberger TD, Greer C *et al.* Microbial diversity of active layer and permafrost in an acidic wetland from the Canadian High Arctic. *Can J Microbiol* 2011;**57**:303–15.

Wrighton KC, Castelle CJ, Wilkins MJ *et al.* Metabolic interdependencies between phylogenetically novel fermenters and respiratory organisms in an unconfined aquifer. *ISME J* 2014;**8**:1452–63.

Wrighton KC, Thomas BC, Sharon I *et al.* Fermentation, hydrogen, and sulfur metabolism in multiple uncultivated bacterial phyla. *Science* 2012;**337**:1661–5.

Yang S, Wen X, Jin H *et al.* Pyrosequencing Investigation into the bacterial community in permafrost soils along the China-Russia Crude Oil Pipeline (CRCOP). *PLoS One* 2012;**7**:e52730.

Yarza P, Yilmaz P, Pruesse E *et al.* Uniting the classification of cultured and uncultured bacteria and archaea using 16S rRNA gene sequences. *Nat Rev Microbiol* 2014;**12**:635–45.

Yergeau E, Hogues H, Whyte LG *et al.* The functional potential of high Arctic permafrost revealed by metagenomic sequencing, qPCR and microarray analyses. *ISME J* 2010;**4**:1206–14.

Youssef NH, Farag IF, Rinke C *et al.* In silico analysis of the metabolic potential and niche specialization of candidate phylum 'Latescibacteria' (WS3). *PLoS One* 2015;**10**:e0127499.

Zalar P, Gunde-Cimerman N. Cold-adapted yeasts in arctic habitats. In: Buzzini P., Margesin R (eds). *Cold-Adapted Yeasts - Biodiversity, Adaptation Strategies and Biotechnological Significance*. Berlin, Heidelberg: Springer, 2014, 49–74.

Zenklusen Mutter E, Blanchet J, Phillips M. Analysis of ground temperature trends in Alpine permafrost using generalized least squares. *J Geophys Res-Earth* 2010;**115**:F04009.

Zhang T, Barry RG, Knowles K *et al.* Statistics and characteristics of permafrost and ground-ice distribution in the Northern Hemisphere. *Polar Geogr* 2008;**31**:47–68.

Zhang X, Zhao L, Xu S *et al*. Soil moisture effect on bacterial and fungal community in Beilu river (Tibetan Plateau) permafrost soils with different vegetation types. *J Appl Microbiol* 2013;**114**:1054–65.

Zimov SA, Schuur EA, Chapin III FS. Permafrost and the global carbon budget. *Science* 2006;**312**: 1612–3.

Zumsteg A, Bååth E, Stierli B *et al*. Bacterial and fungal community responses to reciprocal soil transfer along a temperature and soil moisture gradient in a glacier forefield. *Soil Biol Biochem* 2013;**61**:121–32.

Zumsteg A, Luster J, Göransson H *et al*. Bacterial, archaeal and fungal succession in the forefield of a receding glacier. *Microb Ecol* 2012;**63**:552–64.